Improvement of Wind Farm Performance by Means of Spinner Anemometry

Troels F Pedersen, Giorgio Demurtas, Julia Gottschall, Jørgen Højstrup, Jesper Degn Nielsen, Wolfgang Christiansen, Günther Weich, Anders Sommer,

Friis Pedersen, Troels; Demurtas, Giorgio; Gottschall, Julia; Højstrup, Jørgen; Degn Nielsen, Jesper ; Christiansen, Wolfgang; Weich, Günther; Sommer, Anders; Kristoffersen, Jesper Runge

Publication date:
2013

Document Version
Publisher's PDF, also known as Version of record

DTU Vindenergi

Improvement of Wind Farm Performance by Means of Spinner Anemometry

DTU Vindenergi Report 2014

Troels F Pedersen, Giorgio Demurtas, Julia Gottschall, Jørgen Højstrup, Jesper Degn Nielsen, Wolfgang Christiansen, Günther Weich, Anders Sommer, Jesper Runge Kristoffersen

DTU Wind Energy E-0040

December 2013

DTU Vindenergi
Institut for Vindenergi

Authors: Troels F Pedersen, Giorgio Demurtas, Julia Gottschall, Jørgen Højstrup, Jesper Degn Nielsen, Wolfgang Christiansen, Günther Weich, Anders Sommer, Jesper Runge Kristoffersen

Title: Improvement of wind farm performance by means of spinner anemometry

Abstract (max 2000 char.):

This report is a project report on the EUDP research project SpinnerFarm. The objectives of the project were to improve software and hardware on the spinner anemometer concept and to demonstrate improvement of wind farm performance by opitmized yaw control. The hardware was improved by a more powerful microprocessor and heating was added to the sonic sensor arms plus a range of smaller redesigns. Software was revised with an improved internal calibration procedure. The improved system was tested on a 2MW wind turbine at Tjæreborg wind farm. Measurements on this turbine includes calibration of K factors, determination of induction in center of rotor, measurements of yaw error, inflow angles and turbulence intensity, and measurements of power performance, comparing the spinner anemometer with the mast cup anemometer and the nacelle anemometer. A statistic of yaw error measurements were made in the Vedersø Kær wind farm on nine wind turbines. Finally, estimates of potential power performance gain on the wind farm and the test wind turbine by optimized yaw error measurements was made.

DTU Wind Energy E-0040
December 2013

Contract no.:
EUDP-2009-I
J.nr. 64009-0103

Sponsorship:
Energiteknologisk Udviklings-
Og Demonstrations Program EUDP

Front page:
Spinner anemometer on V80 wind turbine at Tjæreborg

ISBN: 978-87-92896-68-1

Pages: 60
Tables: 2
References: 15

Technical University of Denmark
DTU Wind Energy
Frederiksborgvej 399
Building 125
4000 Roskilde
trpe@dtu.dk
www.vindenergi.dtu.dk

Preface

The present summary report is the final report on the EUDP research project “Improvement of Wind Farm Performance by Means of Spinner Anemometry” with the acronym “SpinnerFarm”. The project was financed by EUDP, Energiteknologisk Udviklings- og Demonstrations Program (EUDP-2009-I, J.nr. 64009-0103). The project was implemented in a cooperation consortium. From the start of the project the consortium consisted of DTU, Metek GmbH, Vestas A/S and Vattenfall A/S. During the project Vestas A/S withdraw from the project and ROMO Wind A/S entered the project.

DTU, Risø Campus, October 2013

Troels Friis Pedersen

Content

Abstract

This report is a project report on the EUDP research project SpinnerFarm. The objectives of the project were to improve software and hardware on the spinner anemometer concept and to demonstrate improvement of wind farm performance by opitmized yaw control. The hardware was improved by a more powerful microprocessor and heating was added to the sonic sensor arms plus a range of smaller redesigns. Software was revised with an improved internal calibration procedure. The improved system was tested on a 2MW wind turbine at Tjæreborg wind farm. Measurements on this turbine includes calibration of K factors, determination of induction in center of rotor, measurements of yaw error, inflow angles and turbulence intensity, and measurements of power performance, comparing the spinner anemometer with the mast cup anemometer and the nacelle anemometer. A statistic of yaw error measurements were made in the Vedersø Kær wind farm on nine wind turbines. Finally, estimates of potential power performance gain on the wind farm and the test wind turbine by optimized yaw error measurements was made.

1. Introduction

The spinner anemometer invention was patented in 2004. A first prototype was produced by Metek, based on their Scientific 3D sonic anemometer. Two sets of prototype sonic sensors were manufactured and connected to the standard Scientific sonic sensor box. In cooperation with Siemens a concept test with a spinner anemometer implemented on a 300kW wind turbine spinner was tested in the Velux wind tunnel [1], and the concept was found successful. Based on the wind tunnel tests an algorithm was developed to convert sonic sensor wind speeds [2,3] into horizontal wind speed, yaw error and flow inclination angle. The results were presented for a Danish audience in 2007 [4]. In an EFP project with Siemens the concept was tested on a Siemens 3,6MW wind turbine at Høvsøre test station [5,6], and the results were presented at Risø Vinddag 2008 [7]. From the experiences with the first prototype another prototype set of five units were produced and procedures for installation, and calibration were developed [8,9]. The five prototypes were used for tests on commercial wind turbines, in order to make wind turbine manufacturers interested. At the same time another research project was initiated under the EUDP research foundation focusing on the use of spinner anemometry in wind farm applications in order to make wind farm owners interested. The project, EUDP-2009-I, J.nr.64009-103, has the acronym SpinnerFarm and this report is the final report on this project.

The objective of the project was to further improve on the spinner anemometer concept and to demonstrate improvement of wind farm performance by application of spinner anemometers for yaw control. Wind farm cost efficiency was expected to be improved by 1-3% in flat terrain or offshore, and up to 5% in complex terrain. Improvement of power performance verification was an additional objective that was not met.

The first objective was to test yaw operation of a single wind turbine by connecting a spinner anemometer to the control system and assess yawing capability by means of the spinner anemometer relative to a met mast. It was not made possible to connect the spinner anemometer to the control system of the Vestas V80 wind turbines as planned. Therefore, this part of the project was never implemented.

The second objective was to determine the yawing capability of the existing nacelle anemometers on a row of wind turbines in a wind farm by mounting spinner anemometers for monitoring yaw error through the control systems. This second objective was met. Not by measurements on the offshore Horns Rev 1 wind farm but on the onshore Vedersø Kær wind farm.

The third objective was to determine and demonstrate performance improvements by yawing the wind turbines in the row by means of the spinner anemometers. Due to lack of connection to control systems this objective had to be abandoned.

The fourth objective was to determine improvements of performance verification according to the draft power performance verification standard IEC61400-12-2 CD by means of spinner anemometers. Power performance measurements were made on the Vestas V80 wind turbine at Tjæreborg, but a detailed verification of the IEC standard was not made in the project due to lack of resources.

The fifth objective was to commercialize the spinner anemometer. This was very successful since ROMO Wind acquired the technology in 2011.

2. Product development

The first description of procedures for installation and calibration was described in 2008 [8], and a user manual was made in 2009 [9]. A description of the spinner anemometer technology was collected and described in a report [8] in 2010. Further development of the spinner anemometer concept was made in this project on both the hardware side and on the software side.

2.1 Hardware development

From the experience of the second prototype spinner anemometers some improvements on the spinner anemometer still had to be made by Metek. There were several improvements related to the hardware:

- Better grounding of sonic sensors
- Heating of sonic sensor heads (2mm longer) and sonic sensor tubes
- Longer sonic sensor body
- Longer fittings on spinner to accommodate the longer sonic sensor bodies
- Redesign of accelerometer mounting in sonic sensor body
- New microprocessors in electronic box, with RS-422 communication protocol

The improved spinner anemometer was mounted on the Vestas V80 at Tjæreborg, and in total 11 spinner anemometers were produced. Ten of these were planned to be mounted on the Horns Rev I wind farm. However, it was realised that it was too costly for the project to install and operate the spinner anemometers on the offshore wind turbines. Instead, nine of the sensors were mounted on an on-shore wind farm at Vedersø Kær in Jutland.

2.2 Icing tests on sonic sensor

The spinner anemometer heating system heats the round sonic sensor tube and the piezoelectric element in the sensor head. Tests without heating showed during icing events that icing would build up on a non-heated sensor, see Figure 1.

Figure 1: Ice build-up on non-heated spinner anemometer sonic sensor, left. On the right is shown ice build-up around a heated 2D sonic anemometer during the same event.

2.2.1 Icing wind tunnel

The heating system was tested for icing in the climate wind tunnel at WindGuard in Germany. This wind tunnel was built in 2009 for the purpose of optimising heating systems on meteorological instruments. Icing may occur at high humidity, temperatures below 0°C, and at low wind speeds. The tests on one spinner anemometer sonic sensor were performed at a temperature of -10°C and a wind speed of 5m/s. The icing was formed by injecting sub-cooled water ($3g/m^3$) into the air stream ahead of the test section. A sketch of the climate wind tunnel is shown in Figure 2.

The setup of the sonic sensor is shown in Figure 3. The sonic sensor was mounted in the centre of the wind tunnel on a plate that was mounted on the test section floor. In the roof of the test section is shown the heated 2D sonic for reference wind speed measurements. The test section walls are transparent in order to verify the built up of ice on the instrument.

The tests were made in two steps. Firstly, the heating was turned on before operation and the icing build up was verified over time. Secondly, after all ice was melted on the sonic sensor, the heating was not turned on and the icing build up was again verified over time.

2.2.2 Ice build-up with heating on

The ice build-up for the first test with the heating system on is shown in Figure 4 and in Figure 6.

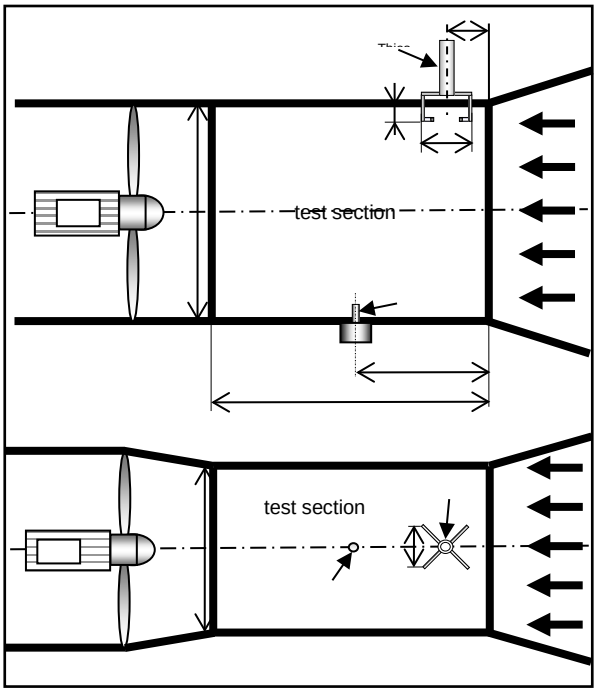

Figure 2: Sketch of icing wind tunnel at WindGuard. Upper sketch as seen from the side, lower sketch as seen from the top. The flow is sucked from the right where also sub-cooled water is injected. The reference heated 2D sonic is shown mounted on the roof.

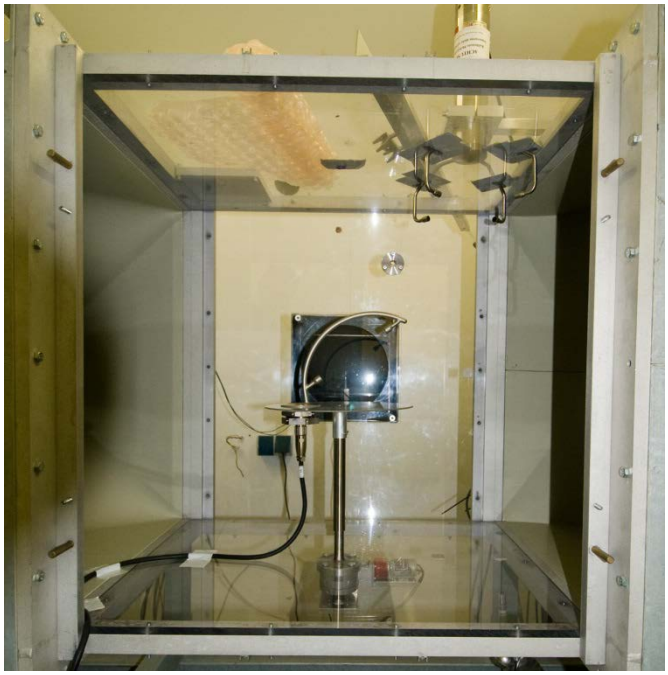

Figure 3 Setup of spinner anemometer sonic sensor in climate wind tunnel with flow from the right. At top is mounted a heated 2D Thies sonic for reference wind speed

Figure 4 First test with heating applied during icing. Left, first visible ice on the lower sensor head after 10min. Right, ice build-up after30min.

In Figure 4 the first ice starts to build up under the lower sensor head. The ice in front of the sensor head is melted and the water flows down under the sensor head where it again freezes. On the right picture in Figure 4 the build-up is seen to have extended down over the sensor head supporting tube and down the round tube to the sonic sensor mounting fitting. On the upper sensor head very little ice build-up is seen. In Figure 6 the ice build-up on the sensor heads is seen in more detail over time. The build-up under the lower sensor head is continued to increase in size and moves forward of the front of the sensor head but still leaving the front surface free of ice. The front of the upper sensor head is also free of ice but some ice has build-up underneath the tube. The heating system was thus able to keep the spinner anemometer running under the icing conditions which lasted for about 1 hour. In these tests the sonic sensor

is fixed with the gravity moving melted ice downwards from the sensor heads. During operation of a spinner anemometer on a rotating wind turbine the gravity will drive the melted ice in all directions and we another build-up pattern might be seen.

2.2.3 Ice build-up without heating

The ice build-up in non-heating conditions is shown in Figure 7. It is seen that the ice is build up on the front of the lower sensor head (which seized the sensor to work) and on the round tube above the sensor head. Over time ice build-up is also shown on the round tube and the sensor head supporting tube below the lower sensor head. On the upper sensor head no ice build-up is seen on the front of the sensor head and relatively little ice build-up is seen on the sensor head supporting tube. The sensor did not work from when the ice covered the front of the lower sensor head and this lasted throughout the test.

Figure 5 shows how the ice build-up covered the whole test setup at the end of the tests.

Figure 5 Melting of ice on the test setup after the second test.

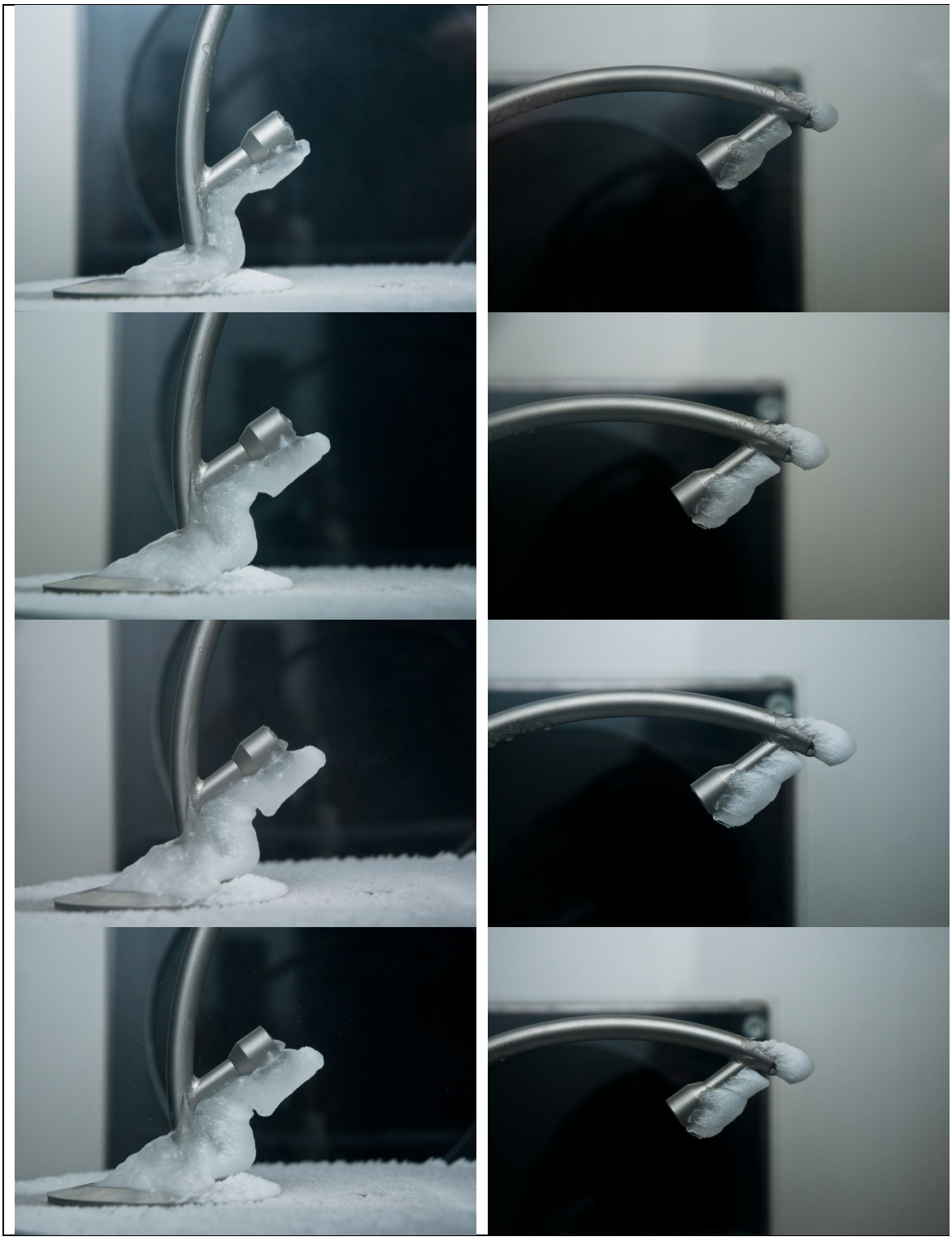

Figure 6 Ice build-up on heated sonic sensor heads on lower (left) and upper (right) sonic sensor heads. From top and down after 40min, 50min, 60min and 70min, respectively.

Figure 7 Ice build-up on non-heated sonic sensor heads on lower (left) and upper (right) sonic sensor heads. From top and down after 20min, 40min, 50min and 60min, respectively.

2.3 Development of internal calibration method

An important part of improvement of the spinner anemometer algorithm was to improve on the internal calibration procedure. This procedure takes account of all deviations in spinner geometry, deviations due to sonic sensor orientation and sonic sensor positioning. The internal calibration ensures that instantaneous measurements are corrected so that the sonic sensors in principle measure the same average wind speed over time. This ensures that turbulence components are measured correctly even with substantial deviations in spinner geometry and mounting.

2.3.1 Introduction

The general assumption of the spinner anemometer algorithm is that the spinner has a perfect geometry, and that geometry of sonic sensors are perfect, and that they are mounted with perfectly the same orientation and position on the spinner. This means that the expressions of the wind speeds in the path of the three sonic sensors positioned on the spinner in the XY'Z' coordinate system are:

$$V_1 = U(K_1 \cos\alpha - K_2 \sin\alpha \cos\theta)$$
$$V_2 = U(K_1 \cos\alpha - K_2 \sin\alpha \cos(\theta - 2\pi/3))$$
$$V_3 = U(K_1 \cos\alpha - K_2 \sin\alpha \cos(\theta - 4\pi/3))$$

Meanwhile, the geometry of spinners is not perfect, sensors are not perfect, and mounting of sensors are not perfect. The K factors may vary individually for the three sensors, though the overall K_1 and K_2 have been found in general from field calibrations. Due to imperfections we have to introduce some correction factors F, which corrects the general K factors to the local sensors to the V' signals that we really measure. Then we have:

$$V_1' = U(K_1 F_{11} \cos\alpha - K_2 F_{21} \sin\alpha \cos\theta)$$
$$V_2' = U(K_1 F_{12} \cos\alpha - K_2 F_{22} \sin\alpha \cos(\theta - 2\pi/3))$$
$$V_3' = U(K_1 F_{13} \cos\alpha - K_2 F_{23} \sin\alpha \cos(\theta - 4\pi/3))$$

Though we have individual differences determined by the F factors we have to require that the wind speed, the flow inclination angle and the general K factors are the same. Thus we have for the general derivation of the wind speed:

$$U = \frac{V_{ave}}{K_1 \cos\alpha} = const$$

So that:

$$V_{ave} = UK_1 \cos\alpha = \frac{1}{3}(V_1 + V_2 + V_3) = \frac{1}{3}(V_1' + V_2' + V_3')$$

2.3.2 Calibrating the F_{1x} factors

When an internal calibration is made the sensor wind speeds are measured over a certain time, for example 30min. During this time the rotor rotates more than 100 rotations. We assume each sensor measuring a cos value as function of the azimuth angle θ. The average value of each sensor is then an integration over all of these values:

$$\overline{V_1'} = UK_1 F_{11} \cos\alpha$$
$$\overline{V_2'} = UK_1 F_{12} \cos\alpha$$

$$\overline{V_3^{'}} = UK_1F_{13}\cos\alpha$$

And:

$$\overline{V_{ave}} = \frac{1}{3}(\overline{V_1^{'}} + \overline{V_2^{'}} + \overline{V_3^{'}})$$

We can then derive:

$$\overline{V_{ave}} = UK_1\cos\alpha\frac{1}{3}(F_{11} + F_{12} + F_{13})$$

This again leads to:

$$\frac{1}{3}(F_{11} + F_{12} + F_{13}) = 1$$

We can then find the F factors by:

$$F_{11} = \frac{\overline{V_1^{'}}}{UK_1\cos\alpha} = \frac{\overline{V_1^{'}}}{\overline{V_{ave}}} \qquad F_{12} = \frac{\overline{V_2^{'}}}{UK_1\cos\alpha} = \frac{\overline{V_2^{'}}}{\overline{V_{ave}}} \qquad F_{13} = \frac{\overline{V_3^{'}}}{UK_1\cos\alpha} = \frac{\overline{V_3^{'}}}{\overline{V_{ave}}}$$

This means that the F correction factors can be determined from the three average sensor wind speed values measured over the 30min calibration measurements.

2.3.3 Calibrating the F_{2x} factors

The maximum and minimum values measured over the 30min time (assuming consistent cosine functions) gives the following values:

$$V_{1,\max}^{'} = U(K_1F_{11}\cos\alpha + K_2F_{21}\sin\alpha)$$
$$V_{2,\max}^{'} = U(K_1F_{12}\cos\alpha + K_2F_{22}\sin\alpha)$$
$$V_{3,\max}^{'} = U(K_1F_{13}\cos\alpha + K_2F_{23}\sin\alpha)$$
$$V_{1,\min}^{'} = U(K_1F_{11}\cos\alpha - K_2F_{21}\sin\alpha)$$
$$V_{2,\min}^{'} = U(K_1F_{12}\cos\alpha - K_2F_{22}\sin\alpha)$$
$$V_{3,\min}^{'} = U(K_1F_{13}\cos\alpha - K_2F_{23}\sin\alpha)$$

The amplitudes which are the differences between these values are:

$$\Delta V_1^{'} = V_{1,\max}^{'} - V_{1,\min}^{'} = 2UK_2F_{21}\sin\alpha$$
$$\Delta V_2^{'} = V_{2,\max}^{'} - V_{2,\min}^{'} = 2UK_2F_{22}\sin\alpha$$
$$\Delta V_3^{'} = V_{3,\max}^{'} - V_{3,\min}^{'} = 2UK_2F_{23}\sin\alpha$$

We then have:

$$2UK_2\sin\alpha = \frac{\Delta V_1^{'}}{F_{21}} = \frac{\Delta V_2^{'}}{F_{22}} = \frac{\Delta V_3^{'}}{F_{23}}$$

When we also make the requirement that the average sensor difference value shall correspond to the general non-adjusted value:

$$\Delta V_{ave} = \frac{1}{3}(\Delta V_1^{'} + \Delta V_2^{'} + \Delta V_3^{'}) = \frac{1}{3}(\Delta V_1 + \Delta V_2 + \Delta V_3)$$

then we have:

$$\Delta V_{ave} = 2UK_2\sin\alpha\frac{1}{3}(F_{21} + F_{22} + F_{23}) = 2UK_2\sin\alpha$$

This again leads to:

$$\frac{1}{3}(F_{21}+F_{22}+F_{23})=1$$

We can then derive:

$$F_{21}=\frac{\Delta V_1^{'}}{2UK_2\sin\alpha}=\frac{\Delta V_1^{'}}{\Delta V_{ave}} \qquad F_{22}=\frac{\Delta V_2^{'}}{2UK_2\sin\alpha}=\frac{\Delta V_2^{'}}{\Delta V_{ave}} \qquad F_{23}=\frac{\Delta V_3^{'}}{2UK_2\sin\alpha}=\frac{\Delta V_3^{'}}{\Delta V_{ave}}$$

In practice the assumption of a consistent cosine signal is not correct during 30min since the wind speed and direction vary, and we cannot rely on the differences of max and min values. Instead, we can relate them to the relative slope. If we make a "bobble sorting" of all the data from the three sensors and their average value, then we will get a span of data covering the $\Delta V_1^{'}$, $\Delta V_2^{'}$, $\Delta V_3^{'}$, and ΔV_{ave} values. If we then take away the lowest 10% values and the highest 10% values to get rid of the peak variations in wind turbulence, then we end up with sorted data on which we can make a linear regression and find the slope. The gain value or slope from this regression is a much more robust determination of the F factors than found by relying on the max and min delta values as derived from the theoretical considerations.

2.3.4 Application of calibration factors in 3D algorithm

We assume that the sensor signals are distorted by local correction factors F_{xx}. Instead of getting the V_x values we get the $V_x^{'}$ values. Now we are interested in correcting the $V_x^{'}$ values to the correct V_x values. If for instance the F_{11} factor would cause an increase of the measured wind speed by a factor of 1,01 then we would need to correct this value back with a factor of 1/1,01.

The internal calibration cannot be applied by a simple correction of the sonic sensor wind speeds. Instead the following procedure must be used. A correction can be calculated by determining first the flow values U, α, φ from the general 3D conversion algorithm with the $V_x^{'}$ values without F factor corrections. With these flow values we calculate what the corrected sensor speeds would be with the F factor corrections:

$$V_{1C}'=U(K_1F_{11}\cos\alpha-K_2F_{21}\sin\alpha\cos\theta)$$
$$V_{2C}'=U(K_1F_{12}\cos\alpha-K_2F_{22}\sin\alpha\cos(\theta+2\pi/3))$$
$$V_{3C}'=U(K_1F_{13}\cos\alpha-K_2F_{23}\sin\alpha\cos(\theta+4\pi/3))$$

The deviations from the measurements are found as:

$$\Delta V_{1C}=V_1^{'}-V_{1C}^{'}=U(K_1(1-F_{11})\cos\alpha-K_2(1-F_{21})\sin\alpha\cos\theta)$$
$$\Delta V_{2C}=V_2^{'}-V_{2C}^{'}=U(K_1(1-F_{12})\cos\alpha-K_2(1-F_{22})\sin\alpha\cos(\theta+2\pi/3))$$
$$\Delta V_{3C}=V_3^{'}-V_{3C}^{'}=U(K_1(1-F_{13})\cos\alpha-K_2(1-F_{23})\sin\alpha\cos(\theta+4\pi/3))$$

These deviations are now applied to the measured sensor wind speeds to get to the V_x values:

$$V_1=V_1^{'}+\Delta V_{1C}=U(K_1(2-F_{11})\cos\alpha-K_2(2-F_{21})\sin\alpha\cos\theta$$
$$V_2=V_2^{'}+\Delta V_{2C}=U(K_1(2-F_{12})\cos\alpha+K_2(2-F_{22})\sin\alpha\cos(\theta+2\pi/3))$$
$$V_3=V_3^{'}+\Delta V_{3C}=U(K_1(2-F_{13})\cos\alpha+K_2(2-F_{23})\sin\alpha\cos(\theta+4\pi/3))$$

These corrected values are now used to find new U, α, θ values based on corrected sensor wind speeds. These new values are eventually only calculated for flow angles where the accuracy is important:

$$0 \le \alpha < 2\pi / 3$$

This last requirement would eventually keep the second loop more simple where back flow is out of the question. A third loop might be used for higher accuracy, but tests showed this not to be necessary.

2.4 Development of calibration method for yaw error measurements

When a spinner anemometer is mounted on a spinner of a new wind turbine type the spinner anemometer constants are normally not known. Meanwhile, data can be acquired with default spinner anemometer constants (for example $K_1 = K_2 = 1$), and later be corrected when calibration factors have been determined. The measured data can be corrected by a precise procedure that does not add correction errors to the measurements. This procedure is more precise than just correcting wind speeds and flow angles linearly with the correction factors.

The precise procedure is schematically shown in Figure 8, where the default values (subscript d) refer to values measured with default calibration coefficients. The principle of the procedure is that the measured wind speeds, yaw errors and flow inclination angles are converted back to the sonic sensor wind speeds with the default K constants, then correcting the K constants with the calibration factors F, and then convert back again to wind speed, yaw error and flow inclination angle. However, it was found that the yaw error and flow inclination angle measurements are only dependent on the ratio between the K_1 and K_2 constants and that it is more convenient to introduce a new constant:

$$K_\alpha = K_1 / K_2$$

The calibrations of the K_1 and K_2 constants are thus more conveniently made on K_α and K_1 by determining the correction factors F_α and F_1.

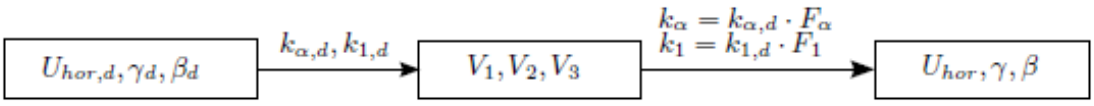

Figure 8 Principle of correct conversion of measured data with default K constants to calibrated values

The expression of the conversion is non-linear which means that averaged values introduce a deviation. As an example, the conversion of a default measured yaw error of 10° and a standard deviation of 5° and with a conversion factor F_α of 0.7 is -0.7% (converted value 14.04° instead of 14.14°). The deviation is +0.3% for an F_α value of 1.3 (converted value 7.748° instead of 7.724°). The deviation seems to be rather constant for different yaw error angles, but is reduced for smaller standard deviations. The deviation increases almost exponentially with the distance of F_α from 1.0. For most cases this deviation is small enough to be neglected, but it should be emphasized that good" guesses of the default K_1 and K_2 constants is advantageous when average values are to be converted.

2.4.1 Calibration method with yawing of the wind turbine

A spinner anemometer was mounted on a Nordtank 500 kW wind turbine. After mounting of the spinner anemometer with sonic sensors and the conversion box, the 4° tilt angle of the rotor shaft and the default K_1 and K_2 constants equal to 1.0 were set in the control box. The internal calibration described in chapter 2.3 was then made according to the operation manual. The yaw error calibration was then made by finding a value for F_α so that the yaw error indicated by the spinner anemometer effectively corresponds to the yaw error.

The method consists of stopping the turbine in a steady and low turbulent wind (> 6 m/s) and yawing the nacelle several times in and out of the wind. The method used fast sampled data (20 Hz). The calibration measurements take about half an hour and do not require a met-mast.

The database of measurements collected during yawing of the wind turbine is then used in an iterative process to calculate the value F_α. The slope of the linear regression between the yaw error measured by the spinner anemometer and the measured yaw position is equal to one when F_α is determined. The figure below shows the calibrated yaw error by the spinner anemometer matching well the yaw error originated by yawing the wind turbine. The variations in the directions are due to turbulence during yawing of the wind turbine.

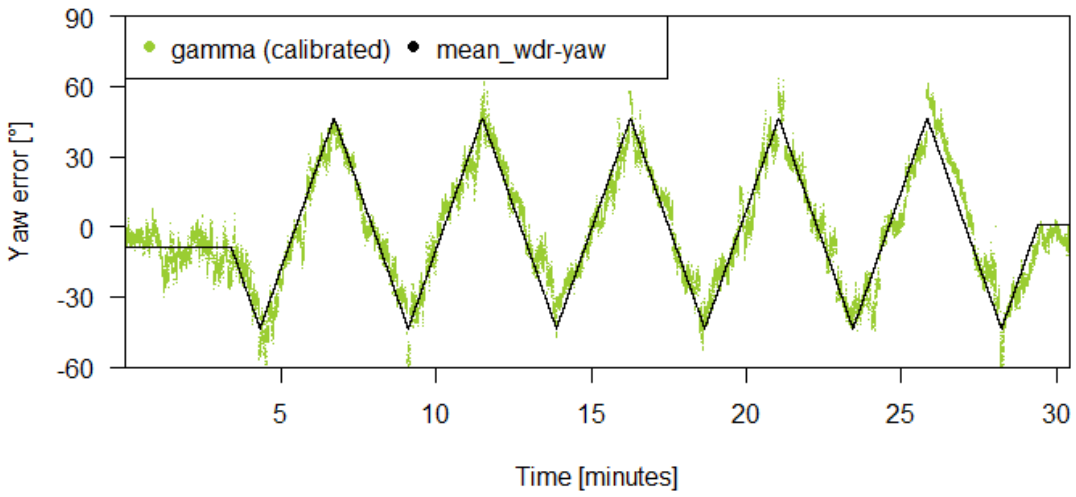

2.4.2 Calibration method with CFD calculations

The wind turbine rotor was modeled with Ellipsys CFD software for a free wind speed of 8 m/s, and for inflow angles of 0º, 10º, 20º, 30º. For each inflow case two simulations were performed, one with rotating rotor, the other with the rotor stopped with blade number one pointed upwards (φ= 0º). This gives eight test cases (rotating/stopped and four inflow angles). For the non-rotating case, only one single rotor position was considered. The tilt angle and the flow inclination angle were set to zero, hence the yaw error correspond to the inflow angle. The CFD simulation gives a set of three velocity components (u; v; w) at each of the three points in space (x; y; z) that corresponds, for each sonic sensor, to the start, the end and the middle of the sonic sensor path (nine points overall). The three-dimensional velocities are projected along the sensor path and averaged for each sonic sensor path. For the rotating case, a full rotor rotation was divided into 2000 steps (0.18º each), and the CFD simulation was repeated for each of them. For the rotating case of φ = 0º the simulation was performed only once, since the wind

speeds at the sensor paths was invariant to the rotor position when the flow was aligned to the spinner axis. In Figure 9 the calculated wind speeds in the paths are shown for an inflow angle of 10°.

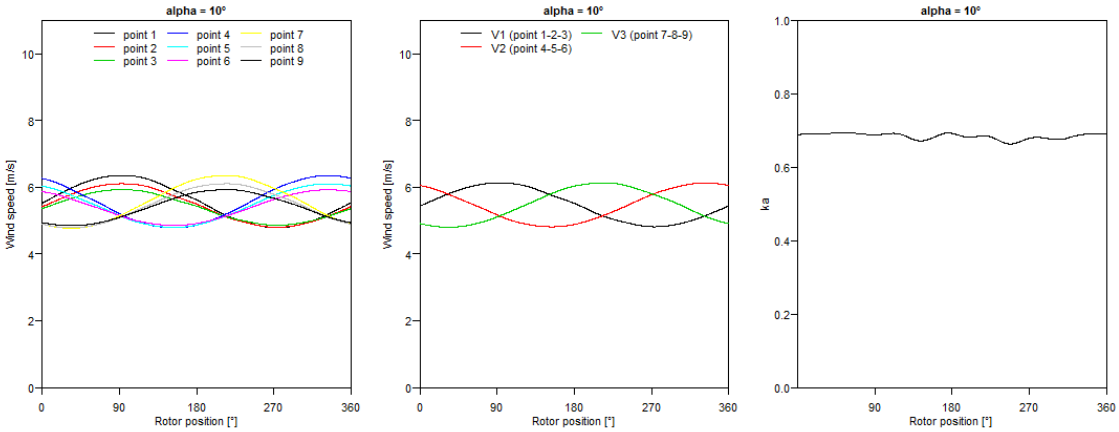

Figure 9 Wind speeds in the sonic sensor paths during one revolution. Left, wind speeds for the three positions in each path; middle, average wind speeds in each path; right, the derived K_α constant

Figure 10 shows a summary of the nine K_α constants for the different flow calculation cases.

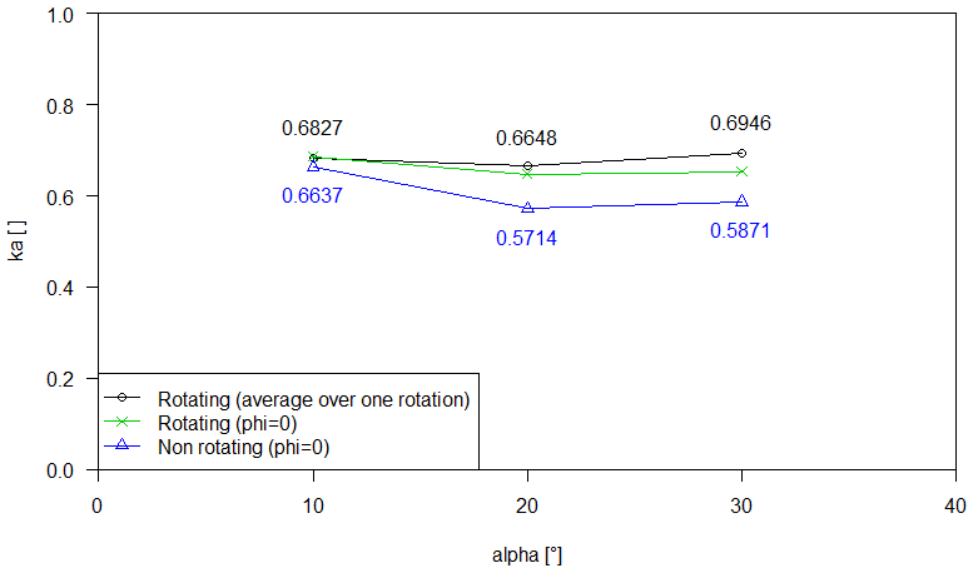

Figure 10 K_α values for the nine flow calculation cases for an inflow angle of 10°

The results for the non-rotating cases of the CFD simulations are included for one azimuthal position (φ= 0) as for the rotating case. The variations in K_α with respect to rotor position makes K_α very dependent on the rotor position chosen for the CFD simulation. The results relative to the rotating cases are probably affected by the induction of the rotor which might influence the wind direction locally at the rotor plane. This effect has not been investigated. However, the general trend of the calculations for different inflow angles that K_α for the non-rotating cases are smaller than for the rotating cases may support the hypothesis that the induced wind speeds due to the rotor induction do increase the yaw errors measured with the spinner anemometer during operation. This is just not supported by experimental data.

2.4.3 Verification of calibration method on NTK500 wind turbine

The experimental and theoretical methods applied to calibrate the K_α constant on the same wind turbine compare within 22%. The CFD calculations seem to give significantly lower K_α values than the experimental determined K_α values. Flow separation may occur for inflow angles higher than 20º due to the pointed spinner, and this may distort the calibrations. The method that seems to be the most reliable is the experimental method of yawing the wind turbine in and out several times in steady wind and during normal operation of the wind turbine.

A sensitivity analysis indicates that the accuracy of yaw error measurements is directly proportional to the accuracy of the calibration constant K_α. This means that a 10% uncertainty on the K_α value gives an uncertainly of 1° on the measurement of 10° yaw error. The hypothesis that yaw error measurement values would be increased from stopped to rotating condition due to the induction of the rotor could not be supported by the experimental determined K_α value because it showed the opposite trend.

3. Field tests on Vestas V80 wind turbine at Tjæreborg wind farm

3.1 Test setup at Tjæreborg wind farm site

The improvements of the spinner anemometer with internal calibration, a heating system and other design changes were implemented on the spinner anemometer mounted on a Vestas V80 wind turbine in the Tjæreborg wind farm, see Figure 11. This wind turbine is an onshore V80 wind turbine, configured exactly like the wind turbines at Horns Rev 1 wind farm, except that it is a 2MW turbine with a hub height of 60m. The rotor diameter is 80m. The onshore wind turbine is located as turbine no 5 in a small wind farm of 8 wind turbines at Tjæreborg, see Figure 12 , all in the same size range as the V80 wind turbine. Coordinates of the wind farm together with the meteorological mast, located 120m or 1.5D (1.5 rotor diameters) southwest of the V80 wind turbine are shown in Figure 13, and relative distances between the wind turbine and directions to the other wind turbines are shown in Table 1. The meteorological mast was 90m high. Cup anemometers and wind vanes were mounted on booms at hub height at 60m. A spinner anemometer [1-4] was mounted on the spinner nose, see Figure 11.

3.2 Measurement database

The measurements were carried out with two separate measurements systems. The first measurement system measured spinner anemometer parameters and mast parameters, measured at 20Hz:

1.	Speed, ave	A 30s moving averaged spinner wind speed value
2.	Yaw, ave	A 30s moving averaged spinner yaw error value
3.	Incl, ave	A 30s moving averaged spinner flow inclination value
4.	Speed	Instantaneous spinner wind speed
5.	Yaw	Instantaneous spinner yaw error
6.	Incl	Instantaneous spinner flow inclination angle
7.	Temp	The sonic air temperature
8.	SpeedQuality	Quality parameter on sonic sensors (all ok=0)
9.	AccQuality	Quality parameter on accelerometer sensors in sensor feet (all ok=0)
10.	CalculationQuality	Quality parameter on rotational speed (operating=0)
11.	Status	Metek box status parameter
12.	Temperature	Mast hub height air temperature
13.	Pressure	Mast hub height air pressure
14.	Cup 7deg	Mast hub height cup wind speed on boom in direction 7deg
15.	Cup 187deg	Mast hub height cup wind speed on boom in direction 187deg
16.	Cup 247deg	Mast hub height cup wind speed on boom in direction 247deg
17.	DAU status	Status of DAU data acquisition unit
18.	A1 Vane 7deg	Mast hub height vane wind direction signal A1 on boom 7 deg
19.	A2 Vane 7deg	Mast hub height vane wind direction signal A2 on boom 7 deg
20.	A3 Vane 247deg	Mast hub height vane wind direction signal A3 on boom 247 deg
21.	A4 Vane 247deg	Mast hub height vane wind direction signal A4 on boom 247 deg
22.	Wind dir 7deg	Mast hub height wind direction on boom in direction 7deg
23.	Wind dir 247deg	Mast hub height wind direction on boom in direction 247deg

The second measurement system measured wind turbine parameters. These were measured with the wind turbine SCADA system at 1Hz:

1. Active parameter A status parameter
2. Active power Electrical power
3. BladePitchAngle Blade pitch angle
4. NacelleDirection Nacelle direction
5. RotorRPM Rotational speed of rotor
6. WindSpeed Nacelle wind speed

The measurements were synchronized with the timestamps in the two data series into a 1Hz database. From the 1Hz database a 30s and a 10min database were derived. The data shown in the analysis are based on data from January 2011 to April 2011. The analysis that relates to hub height wind speed all refer to the cup anemometer on the boom in direction 247°. Errors in data were filtered out. “Frozen” data in WT power and nacelle wind speed were eliminated and only spinner anemometer data with the quality parameter Q000 were used.

3.3 Calibration of spinner anemometer

The output of the spinner anemometer is the local wind conditions at the spinner nose: the horizontal wind speed, the yaw error and the flow inclination angle. During all the tests the two K factors were set equal to the default value, one.

The yaw error of the spinner anemometer is defined as the local wind direction at the spinner minus the nacelle direction. The yaw error was calibrated by yawing the wind turbine in and out of the wind, corresponding to ±90° of spinner anemometer yaw error and 150°-330° yaw direction, see Figure 14. Sampling rate was 1Hz. The calibration factor F_α of the yaw error measurement was found by linear regression of measured data, see Figure 15. The calibration regression resulted in the calibration correction factor $F_\alpha = 1.0227$. This means that all yaw error measurements are multiplied with $1/1.0227 = 0.9778$ to get corrected values.

The wind speed of the spinner anemometer is defined as the local horizontal wind speed at the spinner without the blocking effect of the spinner, blade roots and nacelle. This means, that the measured wind speed for a stopped rotor is the free wind speed, and for at rotor in production, the measured spinner anemometer wind speed is influenced by the general rotor induction in the centre of the rotor. Obviously, the calibration of the wind speed would then best be made relative to a met mast for a stopped rotor. However, it is not appropriate to stop the production of a wind turbine for a longer time in order to calibrate the spinner anemometer. The calibration was therefore made during operation, and in principle following the IEC61400-12-2 standard for establishment of the nacelle transfer function, NTF. During operation the rotor induces a wind speed at the spinner, so that the wind speed at the spinner is reduced compared to the free wind speed. During operation the spinner anemometer then does not measure the free wind but a reduced wind speed dependent on the induction factor. This induction factor is, for a pitch-regulated wind turbine, very little at low wind speeds and at very high wind speeds where the blades are pitched. The calibration value can thus be determined by the ratio of the mast cup wind speed to the spinner anemometer wind speed at low and high wind speeds.

The spinner anemometer was thus calibrated during operation relative to a hub height cup anemometer on a met mast 1.5 rotor diameters away for an open wind direction sector of 212°-252°. Figure 16 shows the cup to spinner anemometer ratio for the un-calibrated spinner anemometer with 10min average data. A linear regression of the data at the highest and lowest wind speeds leads to a calibration correction factor $F_1 = 0.7432$ and the constant $K_1 = K_{1,d} \cdot F_\alpha = 0.7432$. Because the $F_\alpha = 1.0227$ value is very close to 1, and in assuming almost axial flow because the wind turbine is always yawing into the wind, the spinner anemometer conversion algorithm has a linear relationship between the mast wind speed and the spinner wind speed. The spinner anemometer data measured with the default constant $K_{1,d} = 1$ can thus be calibrated by multiplying the data with the factor $1/0.7432 = 1.3455$ to the calibrated wind speed data, see Figure 17. This calibration is equivalent to a calibration with a stopped rotor. The relation between the free mast wind speed and the spinner anemometer wind speed corresponds to the nacelle wind speed transfer function (NTF), described in the IEC61400-12-2 standard. The NTF is in this case simply expressing the induction due to the operating rotor. Figure 18 shows the calibrated spinner anemometer wind speed, corrected with a fitted induction function, see chapter 3.4. It should be mentioned, however, that the mast distance do not meet the requirements in the IEC standard with respect to the distance to the met mast, and with respect to the required measurement data base.

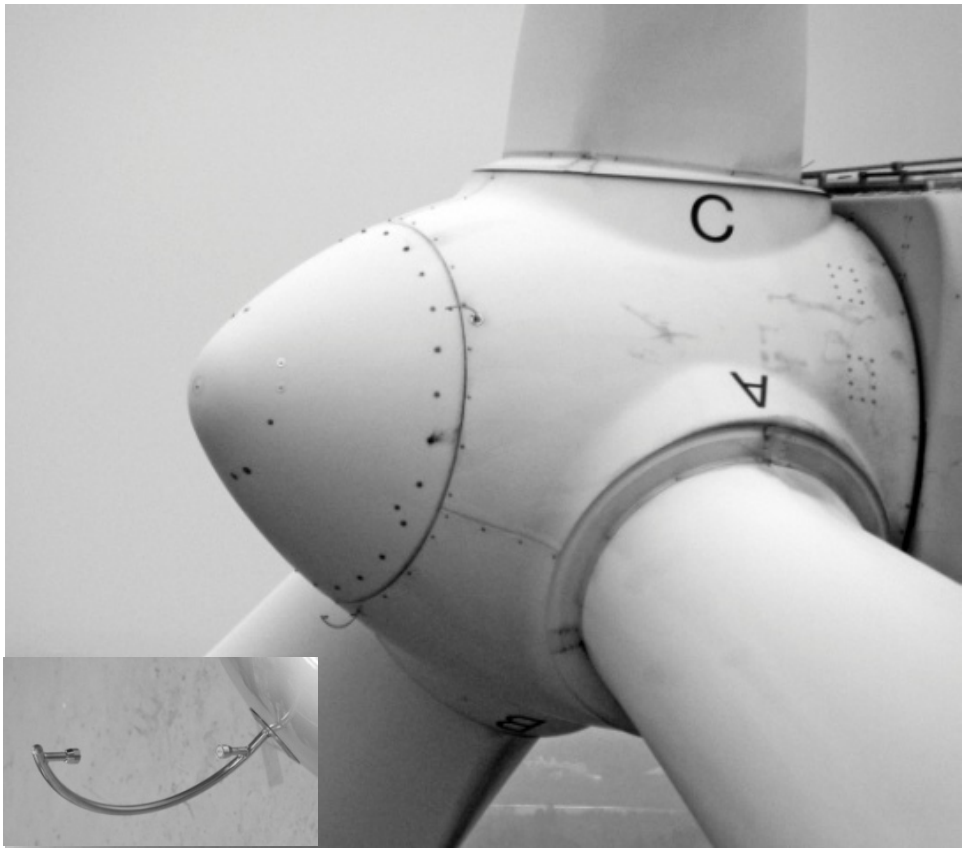

Figure 11 Spinner anemometer mounted on V80 turbine no 5

Figure 12 Tjæreborg wind farm site indicating the positions of the 8 wind turbines and the mast

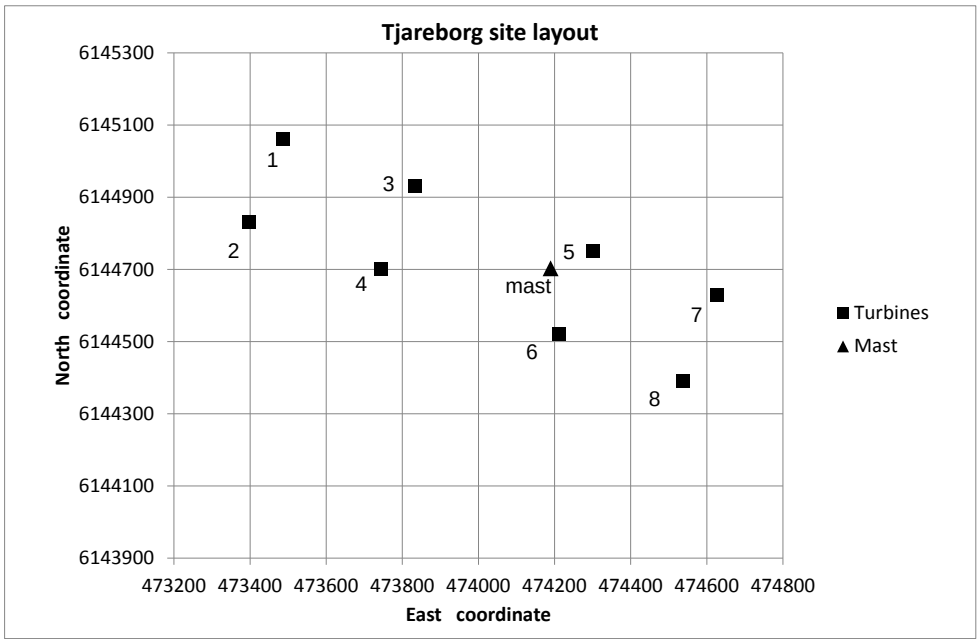

Figure 13 Positions of turbines and mast at the Tjjæreborg wind farm site, the V80 being no. 5

Table 1 Relative distances and directions to wind turbine 5

WT #	Distance to WT #5	Direction to WT #5	Wake lo	Wake hi
	(xD of V80)	(deg)	(deg)	(deg)
1	10,9	291	288	293
2	11,3	275	273	278
3	6,3	291	287	296
4	7,0	265	261	269
5	0,0	-	-	-
6	3,2	201	192	210
7	4,3	110	104	117
8	5,4	147	141	152
WT #	Distance to met mast	Direction to met mast	Wake lo	Wake hi
	(xD of V80)	(deg)	(deg)	(deg)
1	9,8	297	294	300
2	10,0	279	276	282
3	5,3	302	297	308
4	5,6	270	264	275
5	1,5	67	49	85
6	2,3	173	161	186
7	5,5	100	94	105
8	5,8	132	127	137

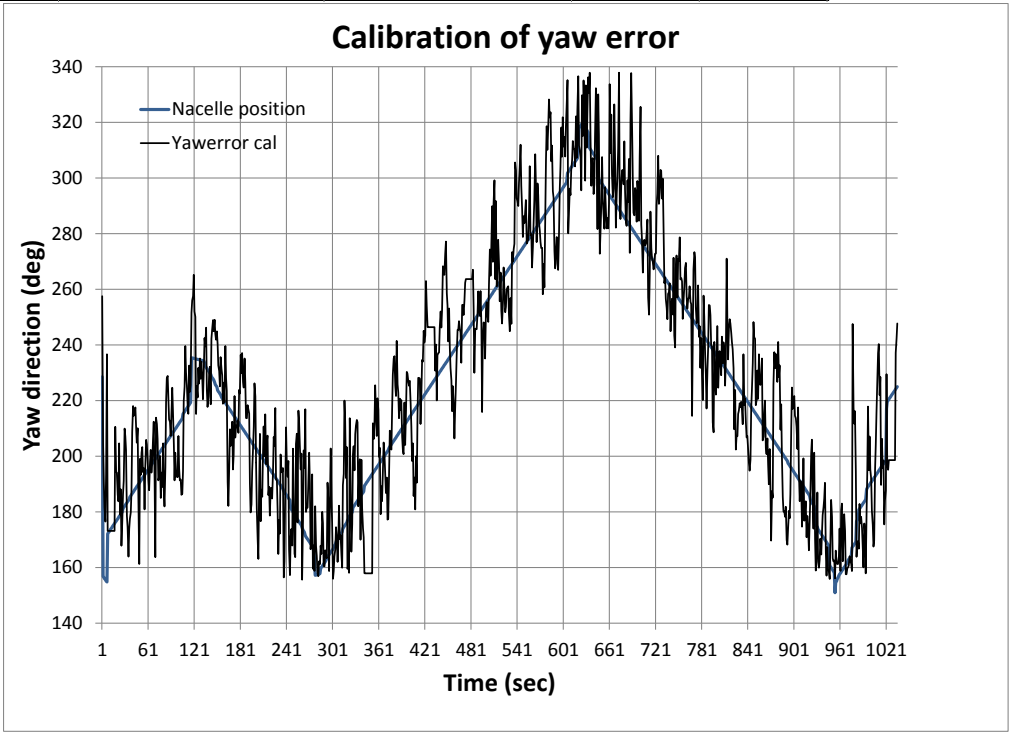

Figure 14 Calibration of yaw error by yawing the turbine in and out of the wind and monitoring at 1Hz. The shown spinner yaw error measurements are calibrated with the linear regression values from the X-Y plot (see Figure 15)

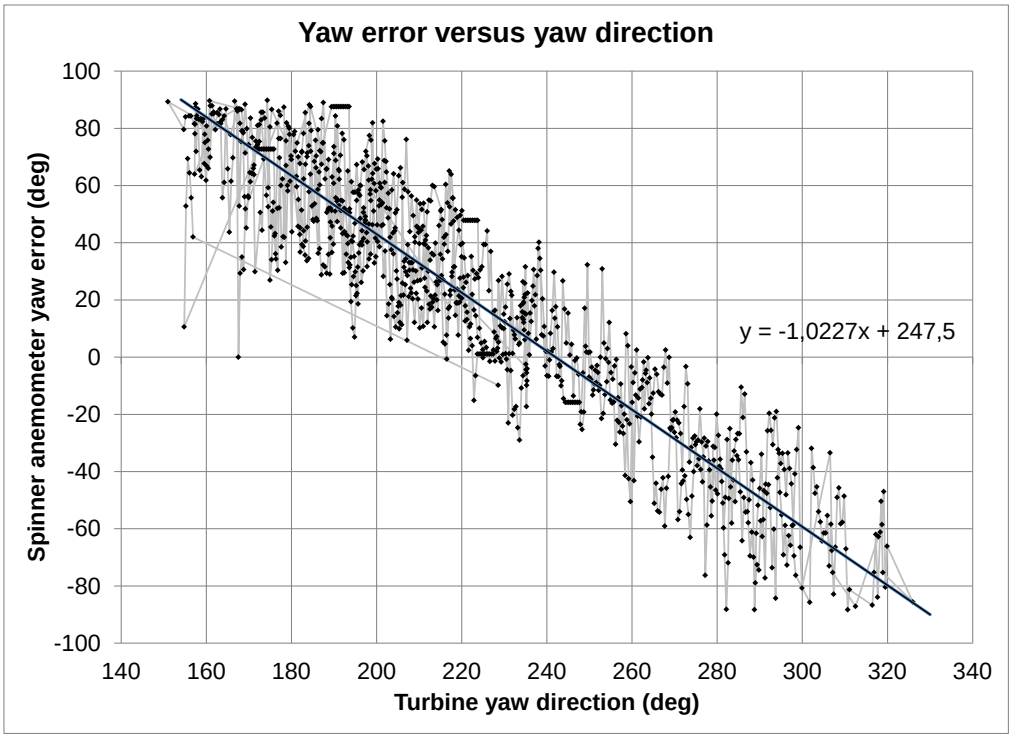

Figure 15 Linear regression of turbine yaw direction versus spinner anemometer yaw error (1Hz data)

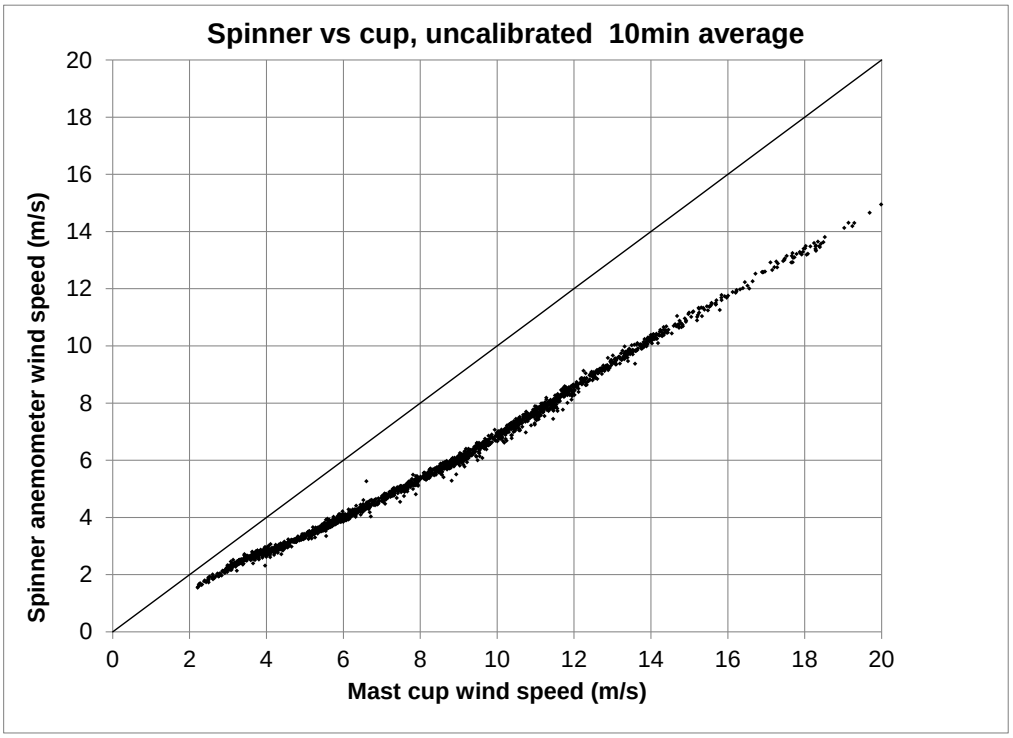

Figure 16 Un-calibrated 10min average spinner wind speeds relative to mast wind speed in free wind sector 212°-252°

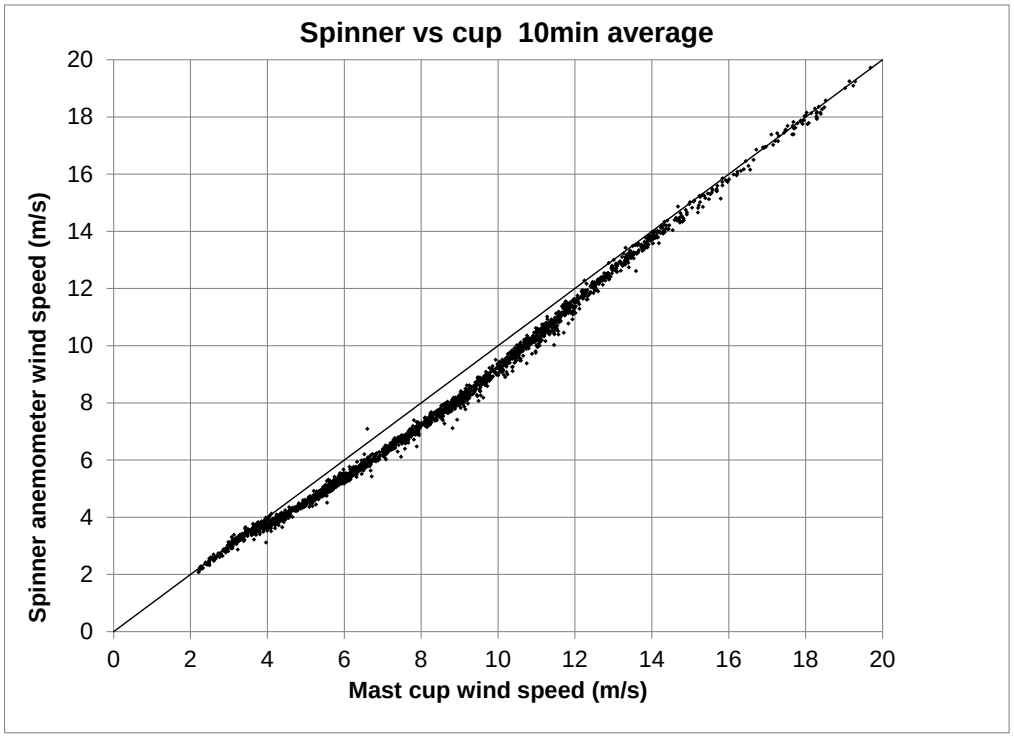

Figure 17 Calibrated 10min average spinner wind speed relative to mast wind speed in free wind sector 212°-252°

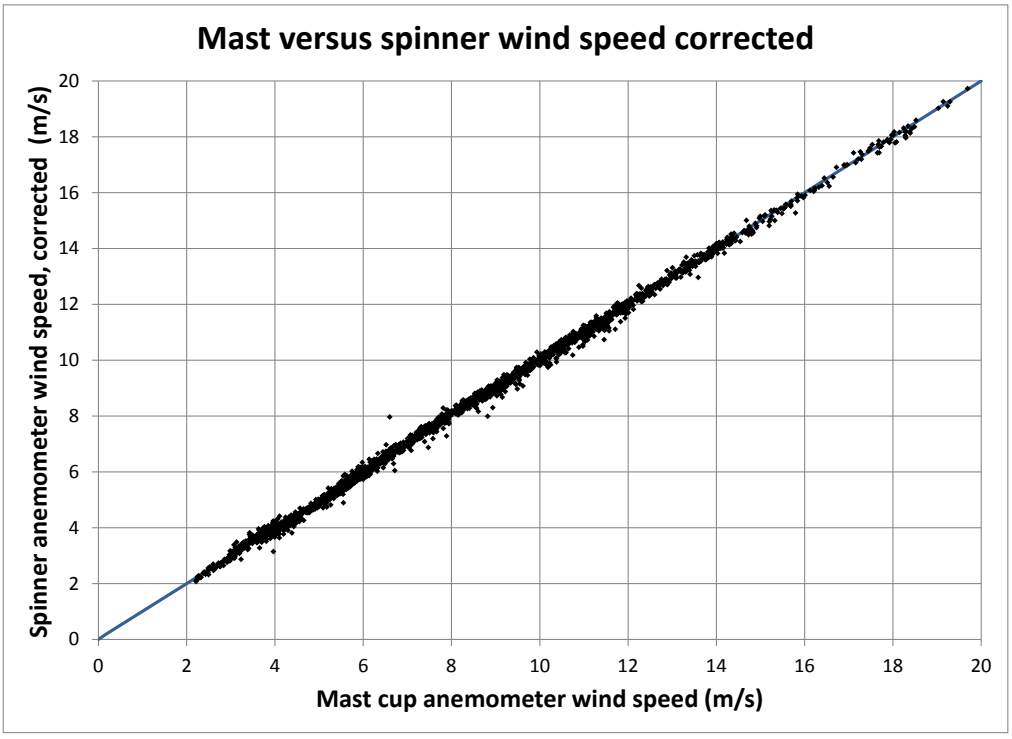

Figure 18 Calibrated and induction corrected spinner wind speed to mast wind speed in free wind sector 212°-252°

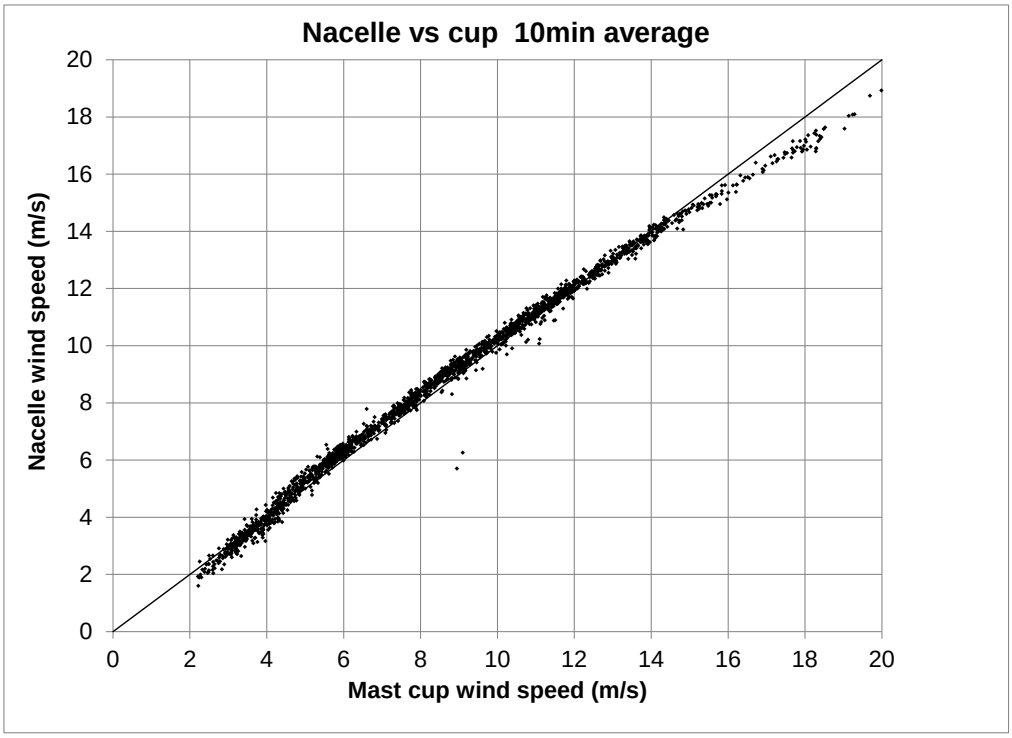

Figure 19 Nacelle 10min average wind speed relative to mast wind speed in free wind sector 212°-252°

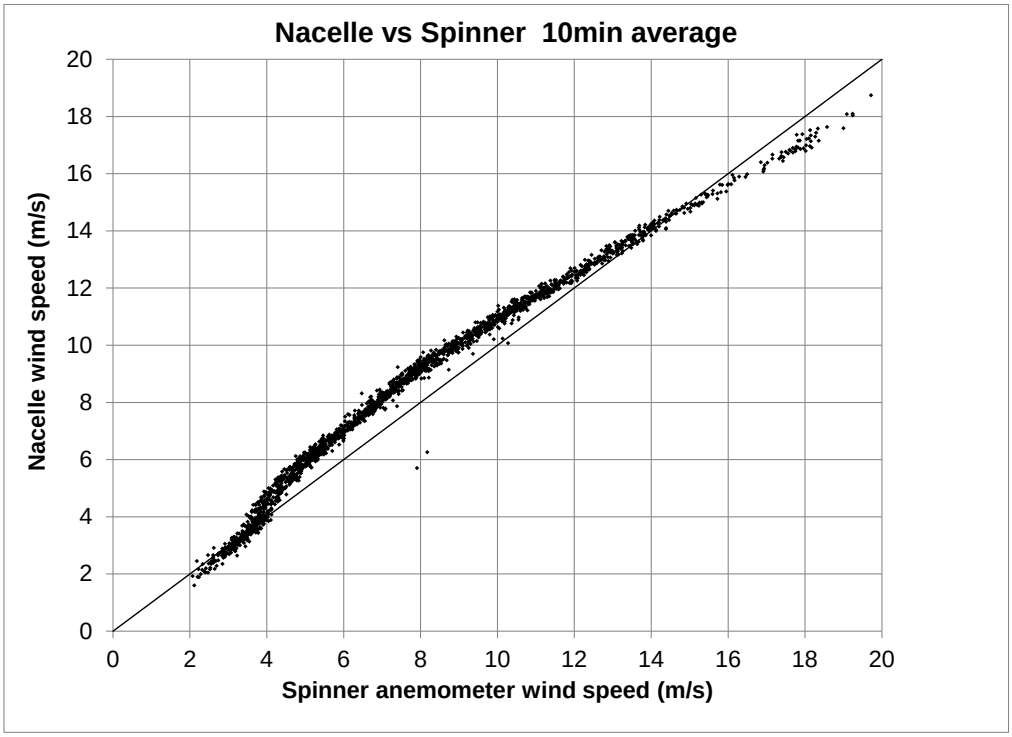

Figure 20 Nacelle 10min average wind speed relative to spinner wind speed in free wind sector 212°-252°

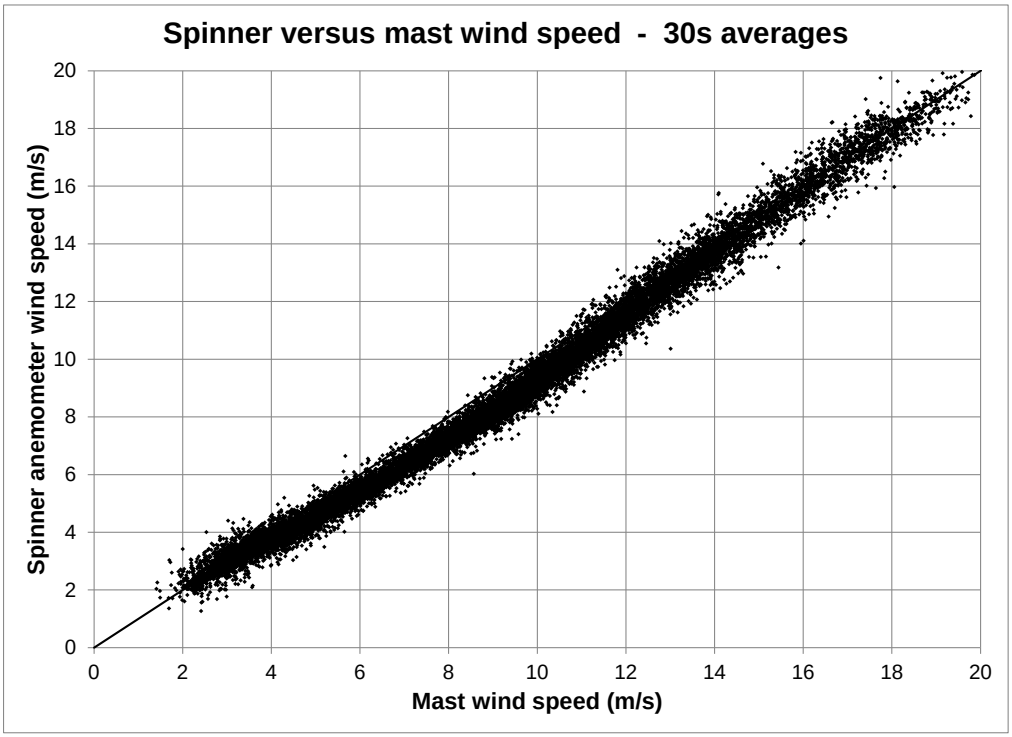

Figure 21 30s average spinner wind speed relative to mast wind speed in free wind sector 212°-252°

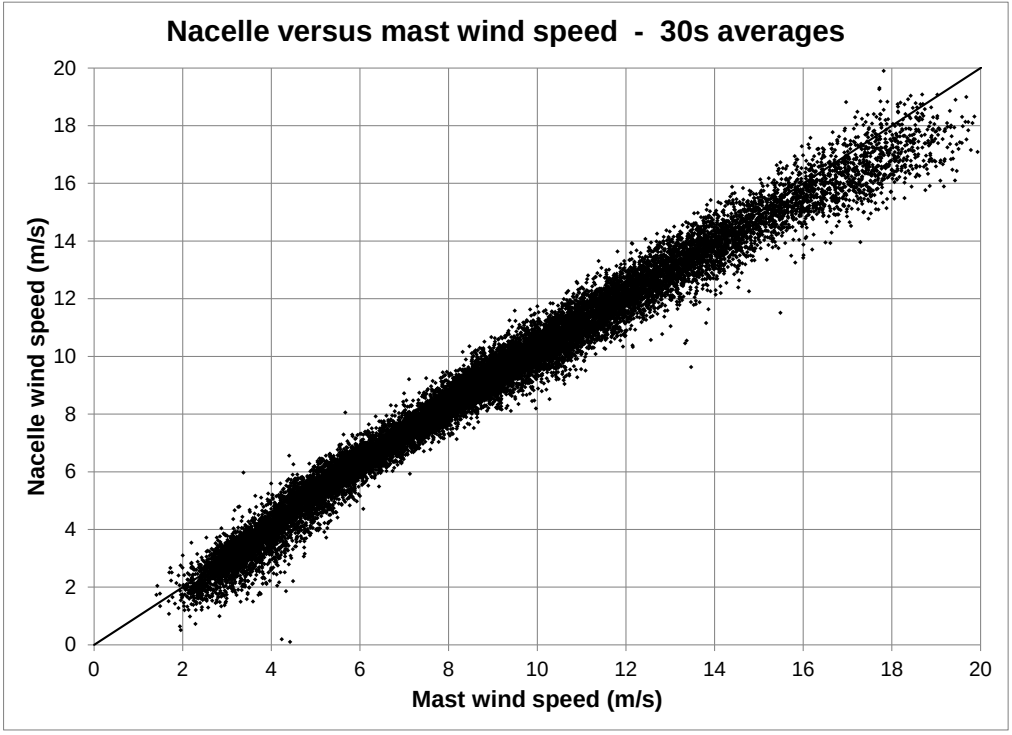

Figure 22 30s average nacelle wind speed relative to mast wind speed in free wind sector 212°-252°

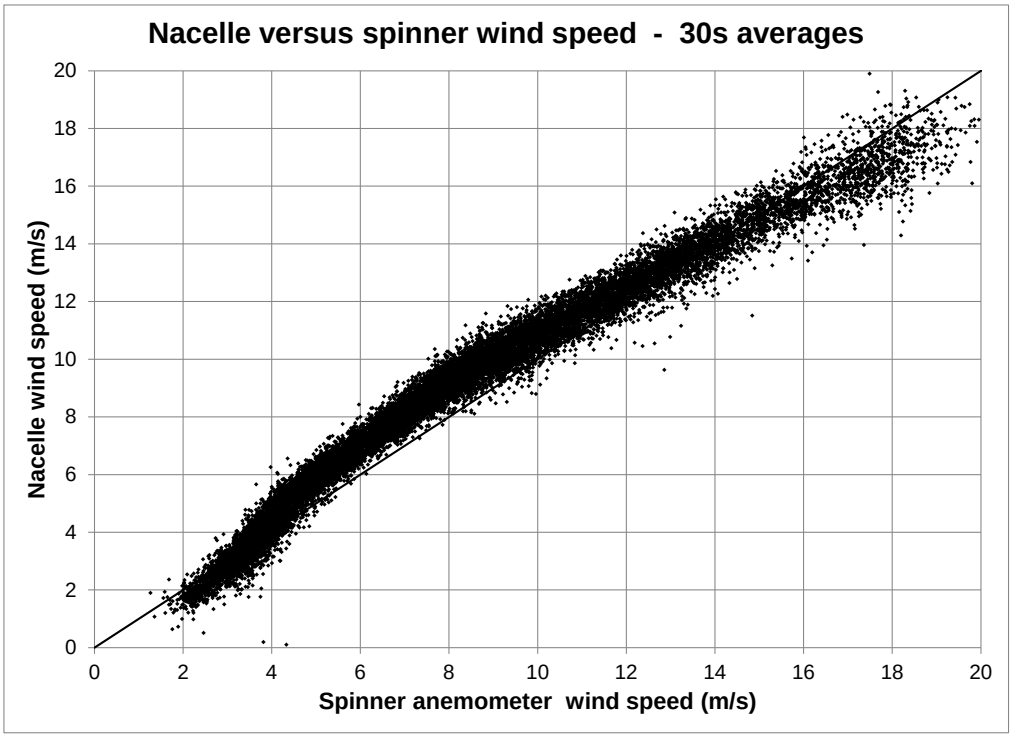

Figure 23 30s average spinner wind speed relative to nacelle wind speed in free wind sector 212°-252°

3.4 Induced wind speed at rotor centre

With the calibration mast measurements the induction factor due to the rotor blades during operation can be determined. Figure 17 shows the spinner anemometer wind speed relative to the met mast cup anemometer with 10min averages. It is clearly seen that the spinner anemometer wind speed is reduced in the range 4-12m/s where the induction due to the thrust of the rotor is most significant. The induced wind speed in the rotor centre, expressed as the induction factor $a = (U_{cup} - U_{sa}) / U_{cup}$, is shown in Figure 24 as function of the mast cup wind speed. Figure 25 shows the induction factor as function of the spinner wind speed. The induction factor is seen to have a maximum value of about 10%. Included in Figure 24 is also a fitted induction function, expressed with the spinner anemometer wind speed:

$$a = B(\frac{U_{sa} - C}{A})^{k-1} \exp(\frac{U_{sa} - C}{A})^{k}$$

The constants are A=5.6, B=0.25, C=3 and k=1.8.

3.5 Wind speed ratio for different wind directions

The ratio between the spinner anemometer and the hub height cup anemometer for all directions is shown in Figure 26. In the figure the directions of the wakes of the turbines on the mast and on the spinner anemometer on the V80 are indicated by coloured labels. Two open sectors, where both turbine No 5 and the meteorological mast are exposed to free flow, 212°-252° and 320°-35°, are shown with a rather constant ratio at about 0.9 (which corresponds well with the induction). The analysis of free flow conditions all refer to the sector 212°-252°. The wake of the closest turbine No 6 on the V80 turbine No 5 in direction 201° and the wake on the mast in direction 173° are clearly seen. Wakes of the other turbines give similar disturbances.

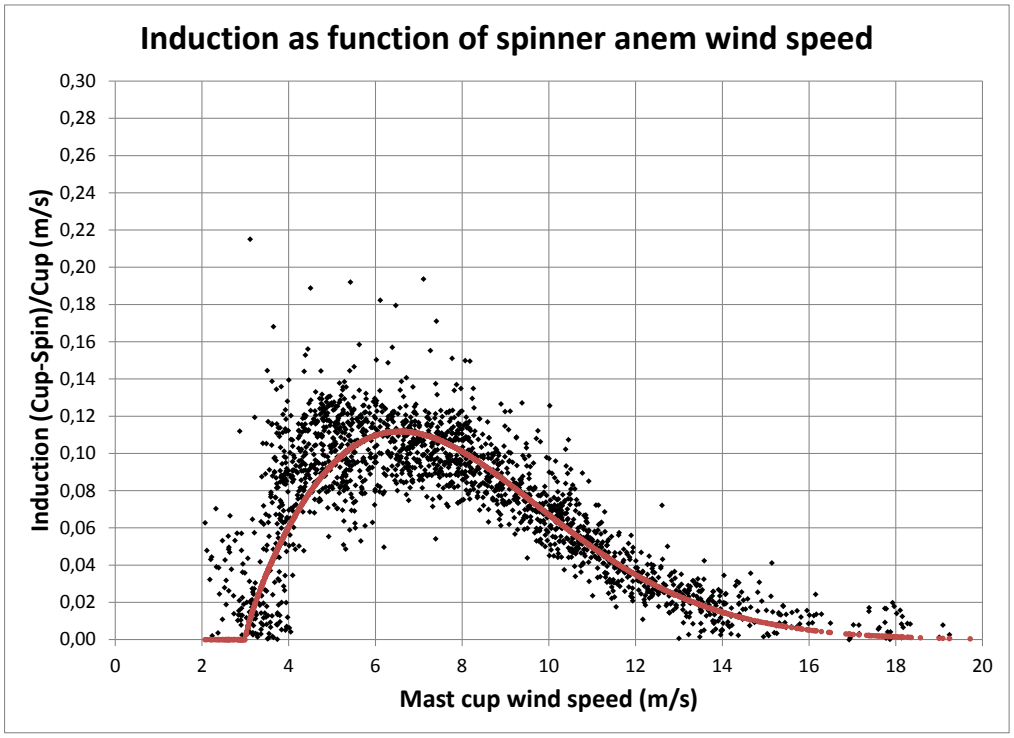

Figure 24 Induction factor as function of mast cup wind speed at rotor centre in free wind sector 212°-252°

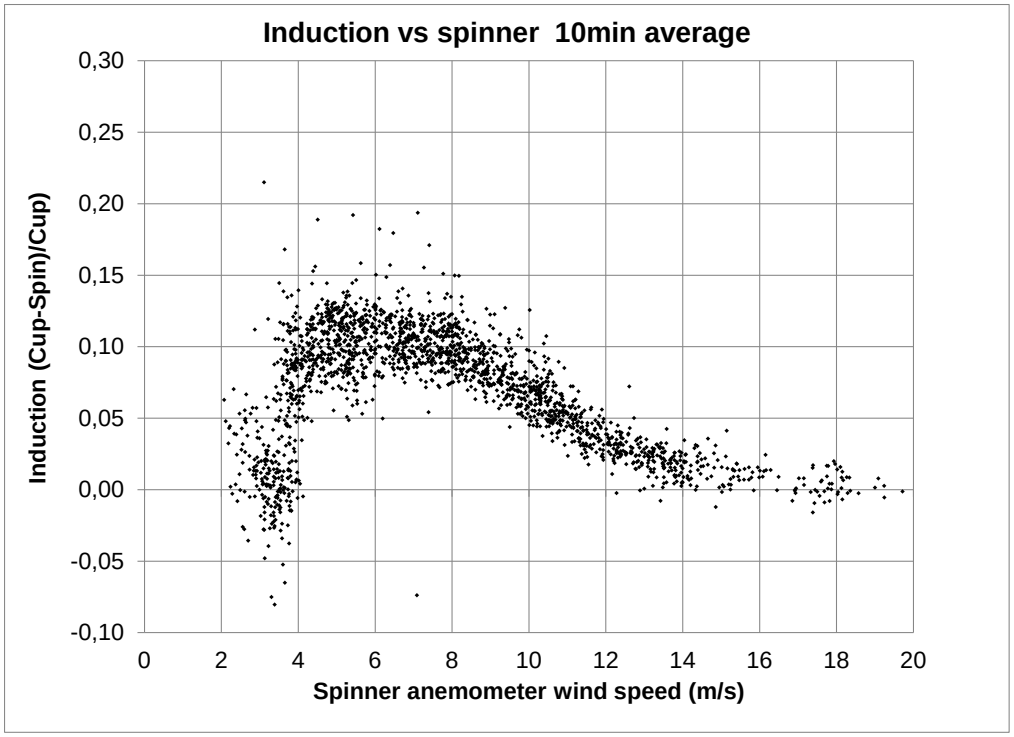

Figure 25 Induction factor as function of spinner anemometer wind speed at rotor centre in free wind sector 212°-252°

3.6 Yaw error

Yaw error measurements with 10min averages for all directions are shown in Figure 27. The yaw error is seen to vary mostly from 0° to 15°with an average value of about 9°, but with a few measurements down to -15°. The yaw error as a function of spinner anemometer wind speed for the free wind direction sector 212°-252° is shown for 10min averages in Figure 29 and for 30s averages in Figure 30. A smaller cloud of data at about -10° is found between 4 and 6m/s for 30s averages. Figure 33 shows the yaw errors measured by the spinner anemometer relative to yaw errors measured by the mast vane and the nacelle direction. The nacelle direction sensor is not calibrated and is seen to have a significant deviation.

3.7 Flow inclination angle

Flow inclination angle measurements with 10min averages for all directions are shown in Figure 28. From most of the directions the flow inclination angle is between 5° and 0°. However, a systematic change of inflow angle is seen in the wake of turbine No 6. At 192° the inflow angle is almost 14° while at 207° the inflow angle is -13°. Between these points there is a linear change of inflow angle. This inflow angle pattern is due to the rotation of the wake of turbine No 6. The wake rotation from turbine No 6 is opposite the rotation direction of the rotor of the wind turbine and this result in an up-flow on the left side of the wake and a down-flow on the right hand side of the wake, seen from the back of the wind turbine. The flow inclination angle as a function of spinner anemometer wind speed is shown for 10min averages in Figure 31 and for 30s averages in Figure 32. A smaller cloud of data at about -8° is found between 4 and 6m/s for 30s averages.

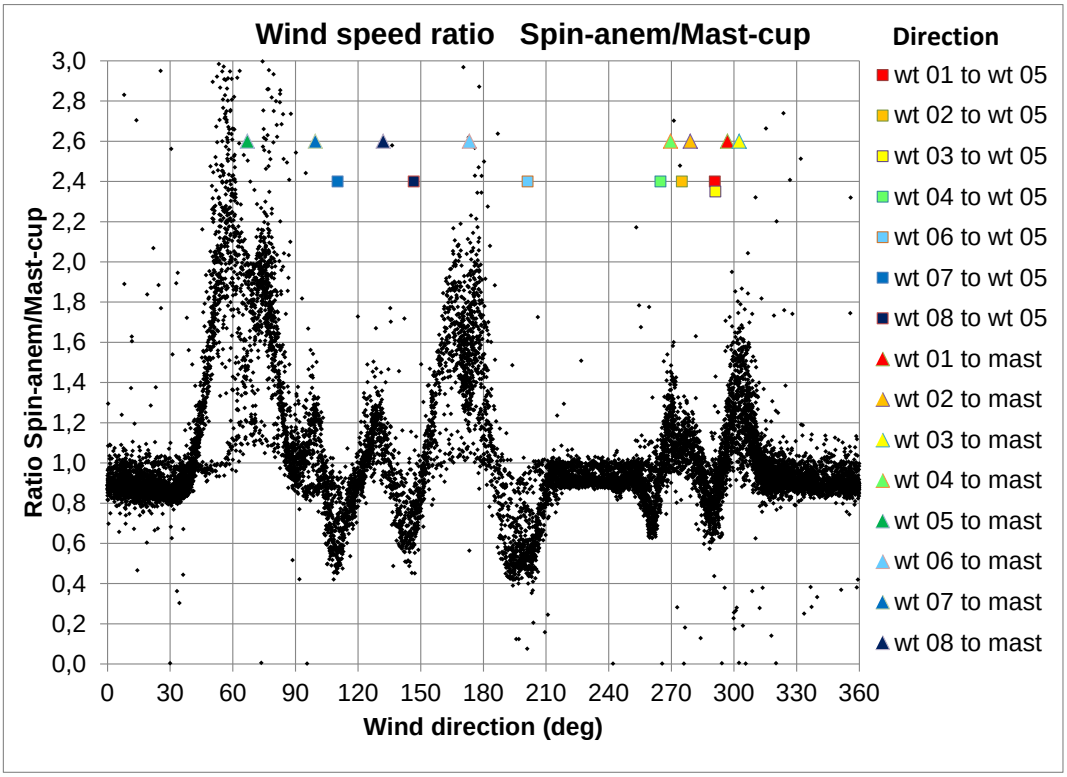

Figure 26 Spinner anemometer wind speed relative to cup wind speed from all wind directions

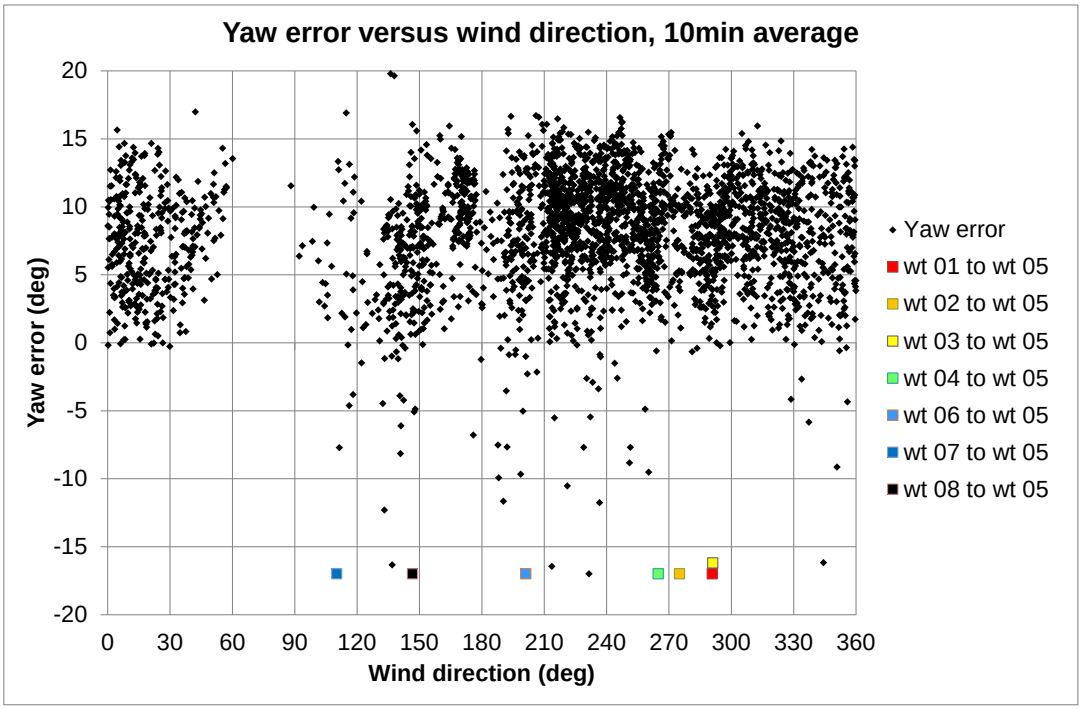

Figure 27 Yaw error with 10min averages from all wind directions

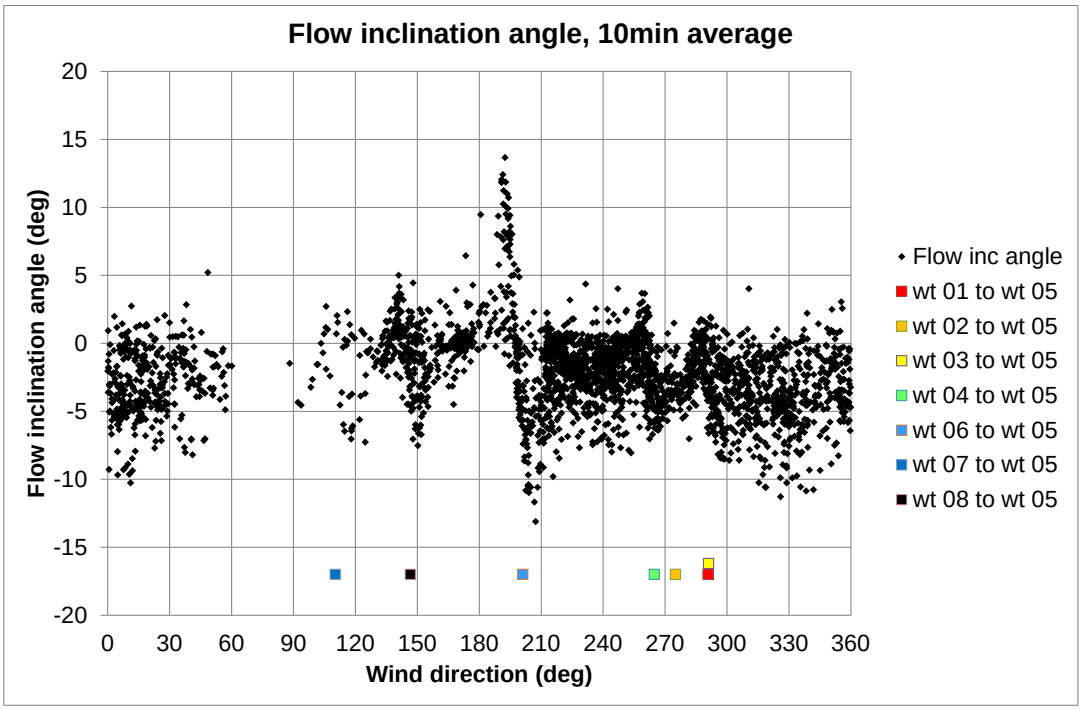

Figure 28 Flow inclination angle with 10min averages from all wind directions

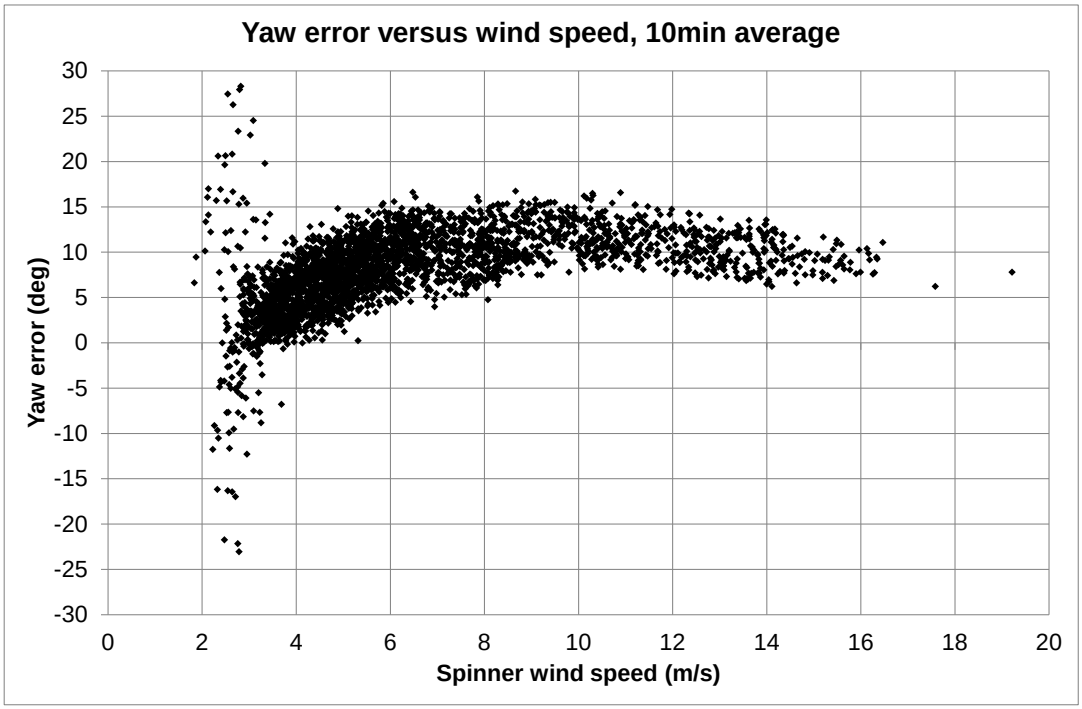

Figure 29 Yaw error as function of wind speed with 10min averages from all wind directions

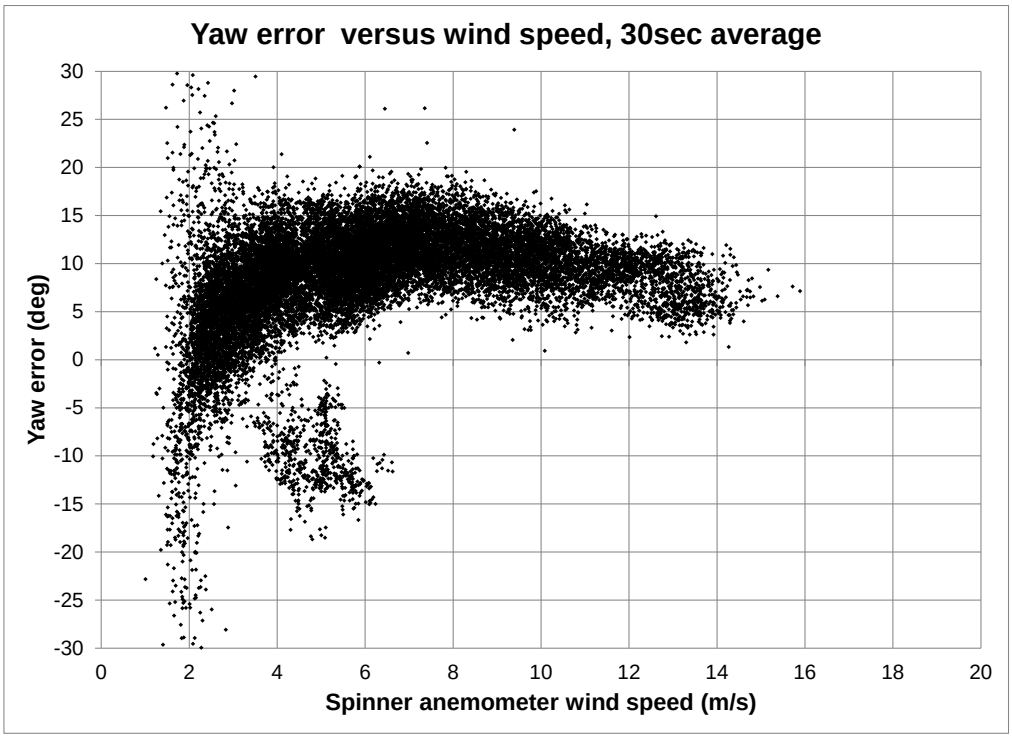

Figure 30 Yaw error as function of wind speed with 30s averages from all wind directions

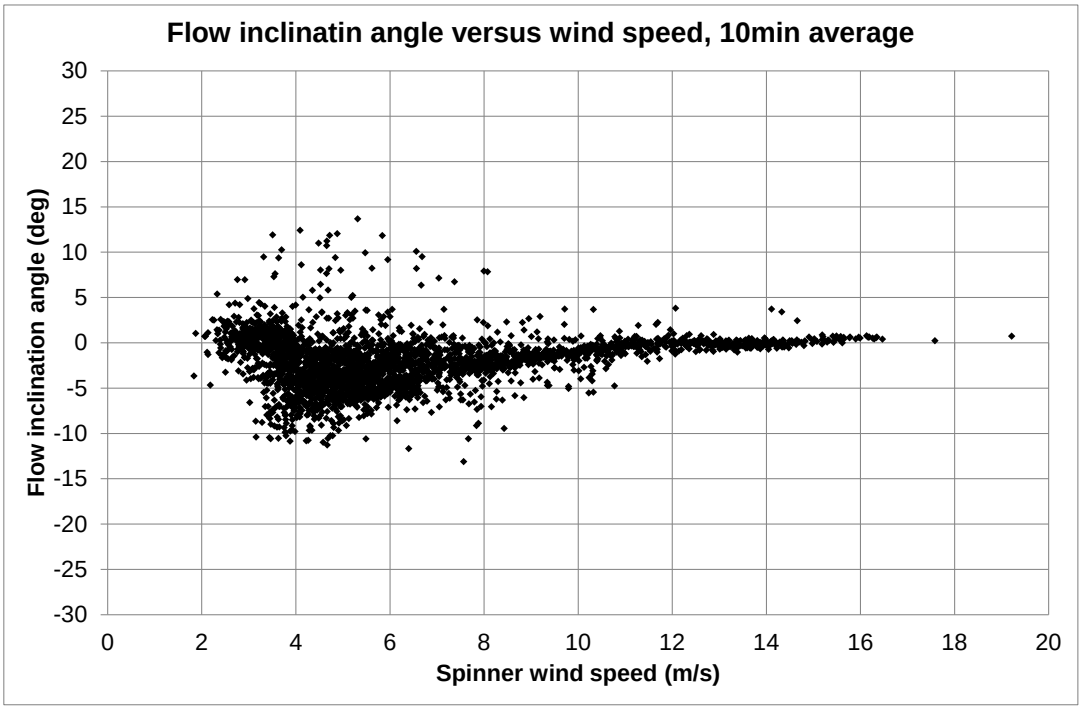

Figure 31 Flow inclination angle as function of wind speed with 10min averages from all wind directions

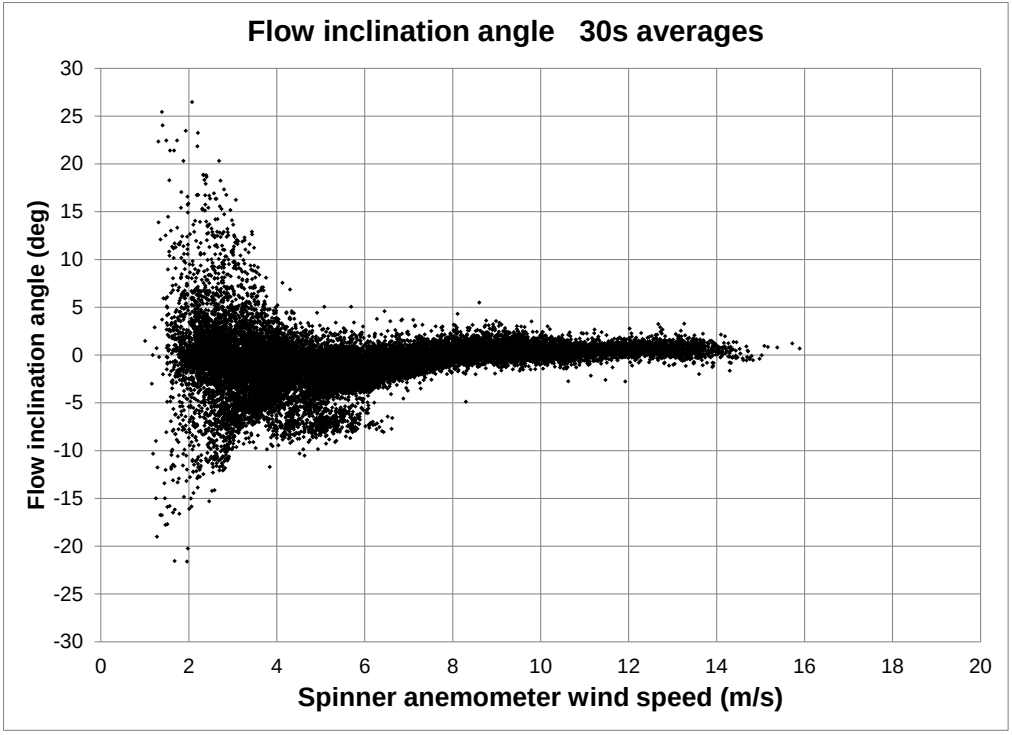

Figure 32 Flow inclination angle as function of wind speed with 30s averages from all wind directions

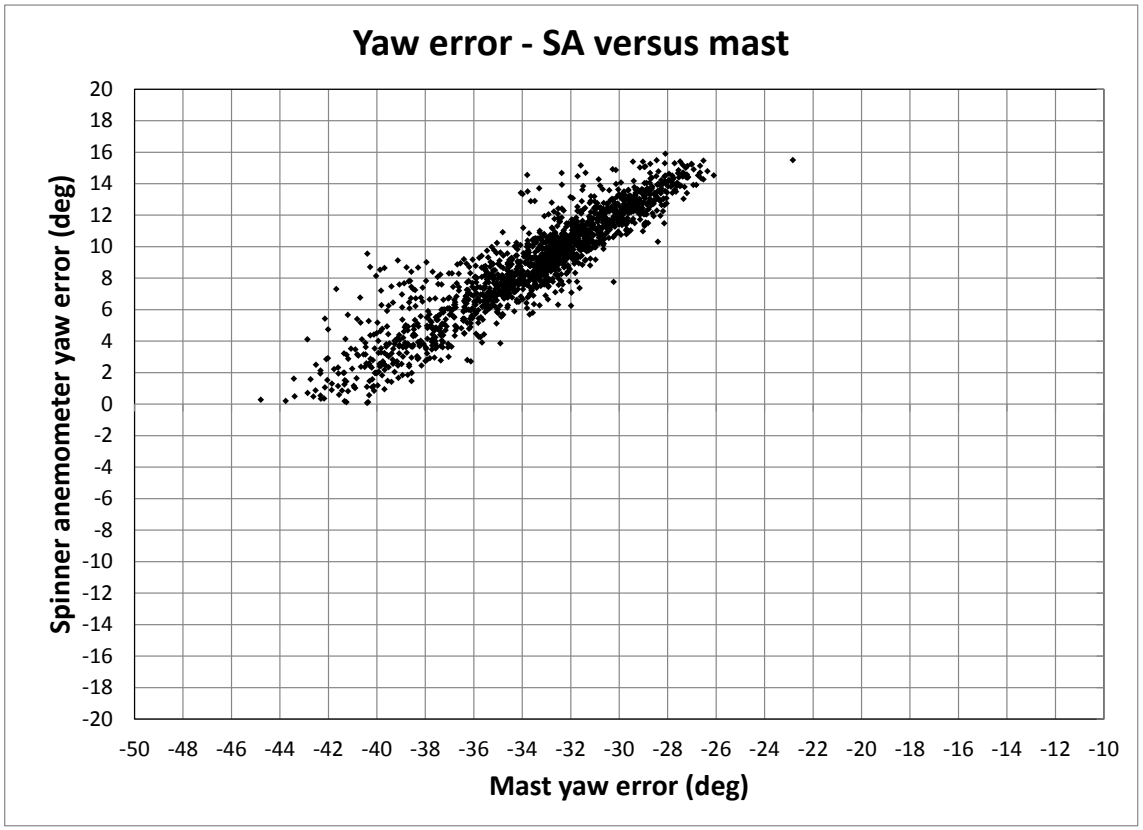

Figure 33 Yaw error measurement of spinner anemometer versus mast measurements

3.8 Turbulence intensity

The turbulence intensity measured by the spinner anemometer related to the turbulence intensity measured by the mast cup anemometer is shown in Figure 34. The relationship shows a rather linear relationship. However, the spinner anemometer measures in general 10% higher turbulence intensity than the cup anemometer. The standard deviations shown in Figure 36 are, meanwhile, very much the same. This indicates that the turbulence vortices are translated through the inflow region of the rotor without being distorted while the average wind speed is being reduced by the induction due to the rotor. Correction of the spinner wind speed to free wind speed with the use of the NTF (the induction function in chapter 3.4) generate a turbulence intensity data set that compare better to the mast cup turbulence, see Figure 35.

Turbulence intensity measured by the nacelle anemometer related to the turbulence intensity measured by the mast cup anemometer is shown in Figure 37. A much higher spreading of the data is seen at low and high turbulence intensities. However, in the range 0,5 to 0,8 the two measurements compare reasonably well in average.

The turbulence intensity measured by the spinner anemometer, the mast cup anemometer and the nacelle anemometer as function of yaw direction is shown in Figure 38, Figure 39 and Figure 40, respectively.

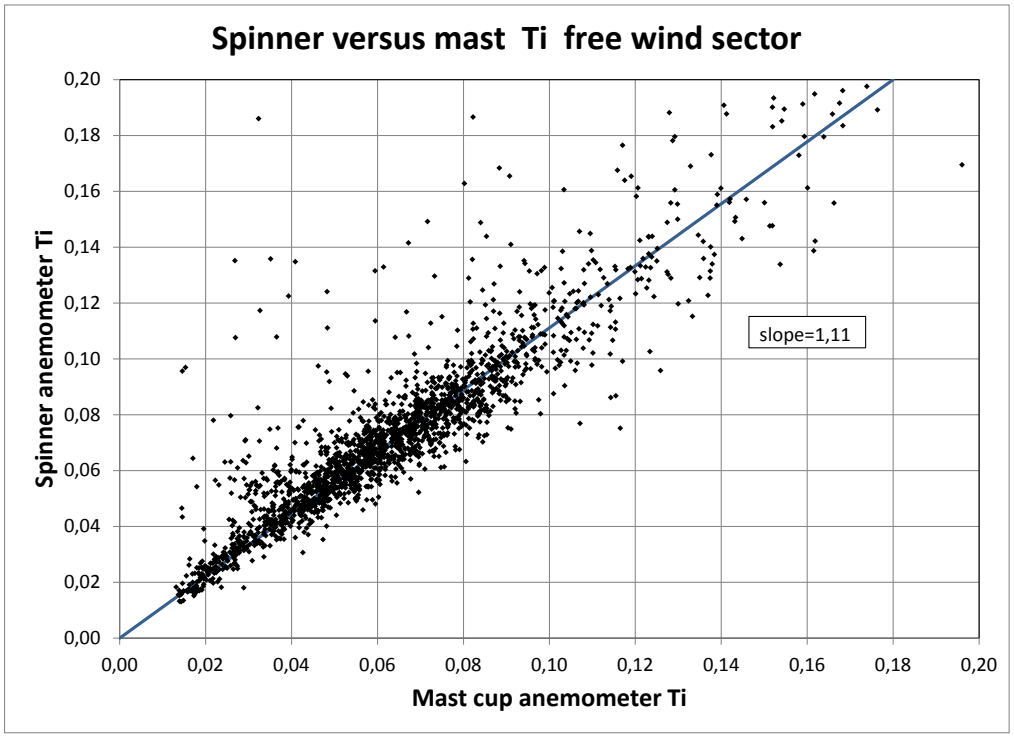

Figure 34 Turbulence intensity of spinner anemometer versus mast cup anemometer in free wind sector 212°-252°. Slope of curve is equal to 1,11.

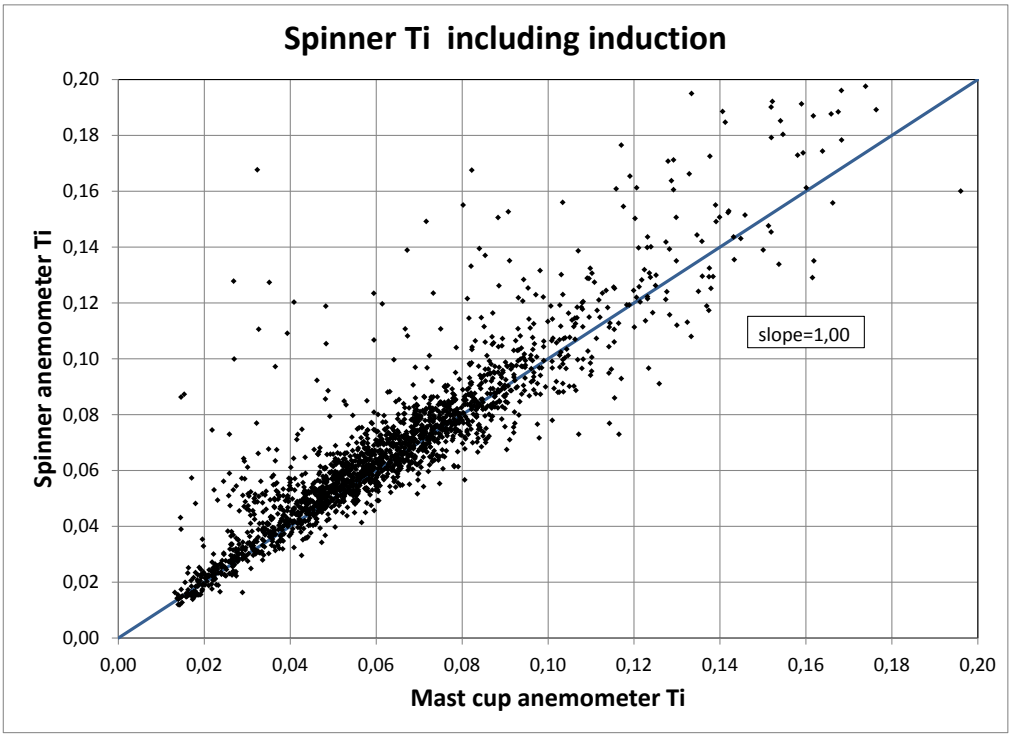

Figure 35 Turbulence intensity of spinner anemometer versus mast cup anemometer in free wind sector 212°-252°. Spinner data are corrected for induction with the induction function, see chapter 3.4.

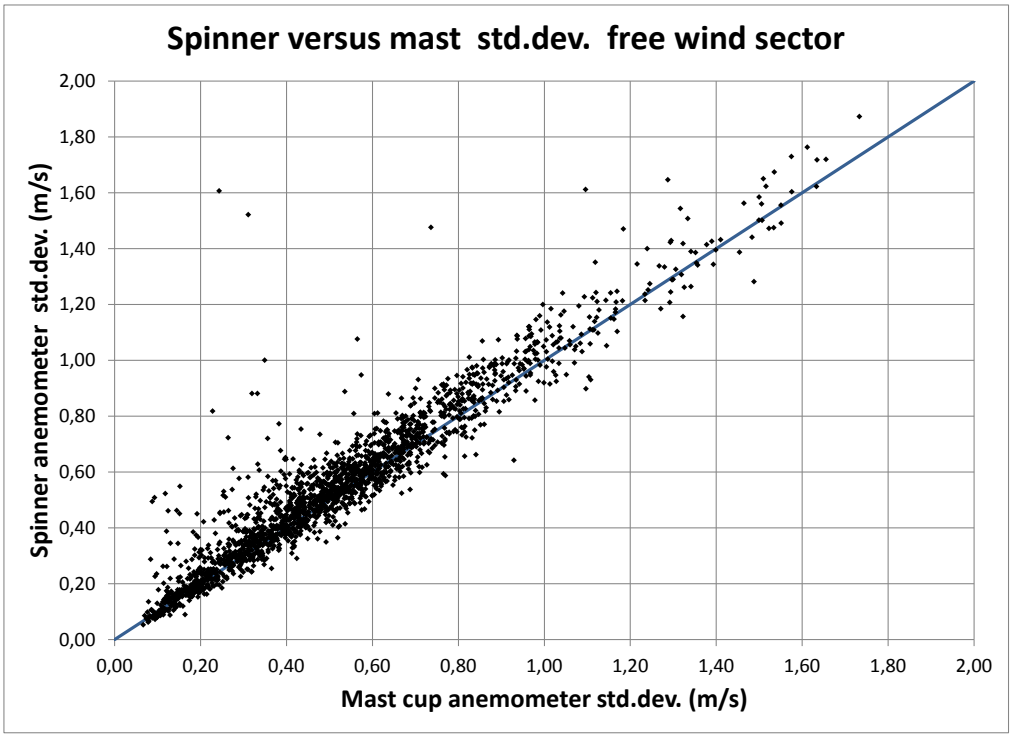

Figure 36 Standard deviation of spinner anemometer versus mast cup anemometer in free wind sector 212°-252°

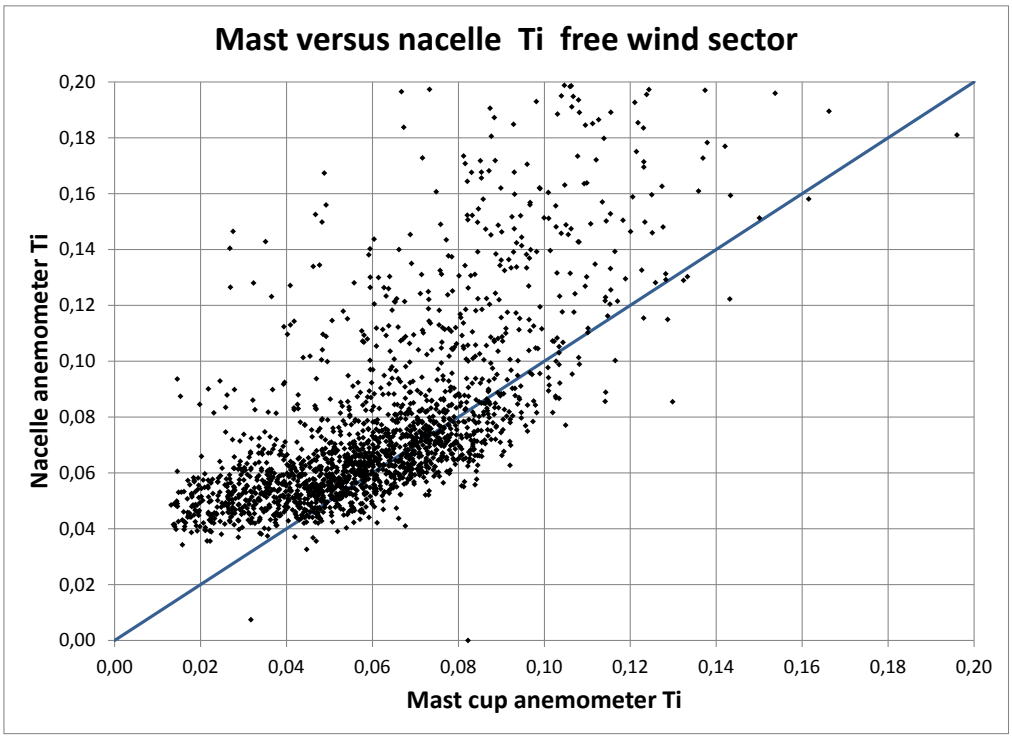

Figure 37 Turbulence intensity of nacelle anemometer versus mast cup anemometer in free wind sector 212°-252°

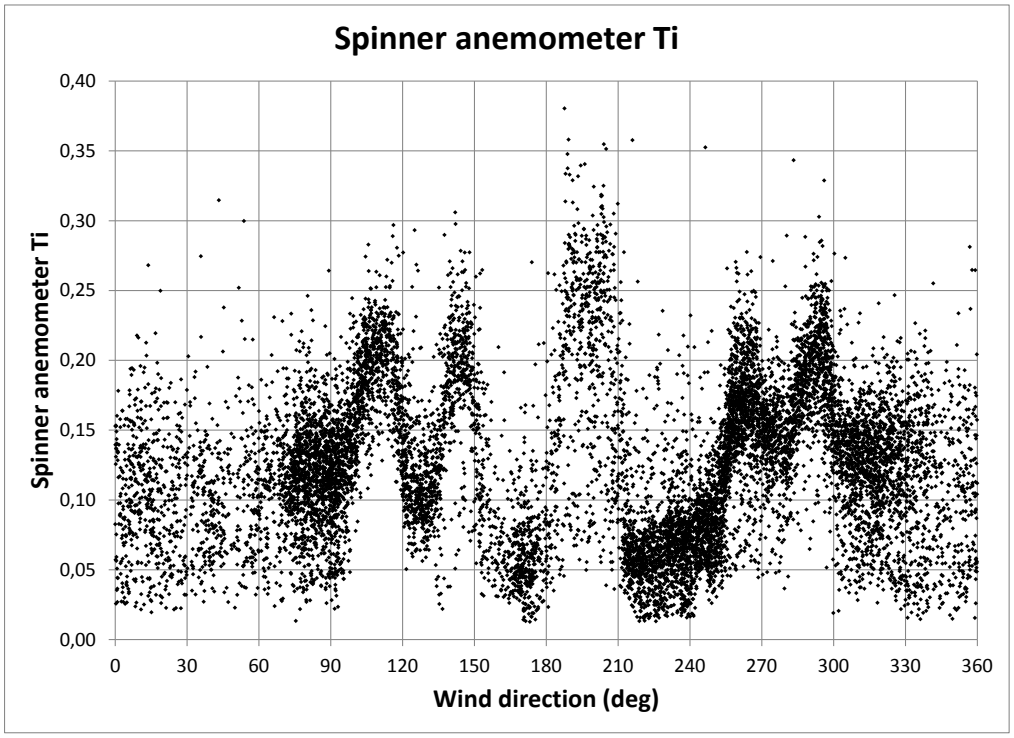

Figure 38 Turbulence intensity measured by spinner anemometer in all directions

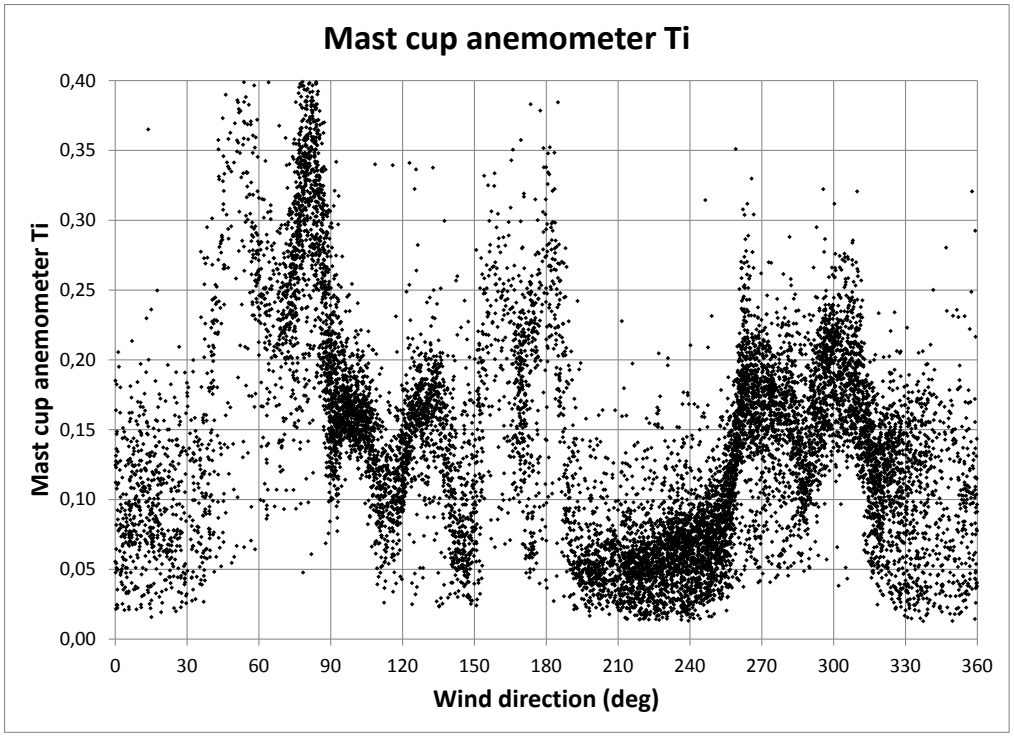

Figure 39 Turbulence intensity measured by mast cup anemometer in all directions

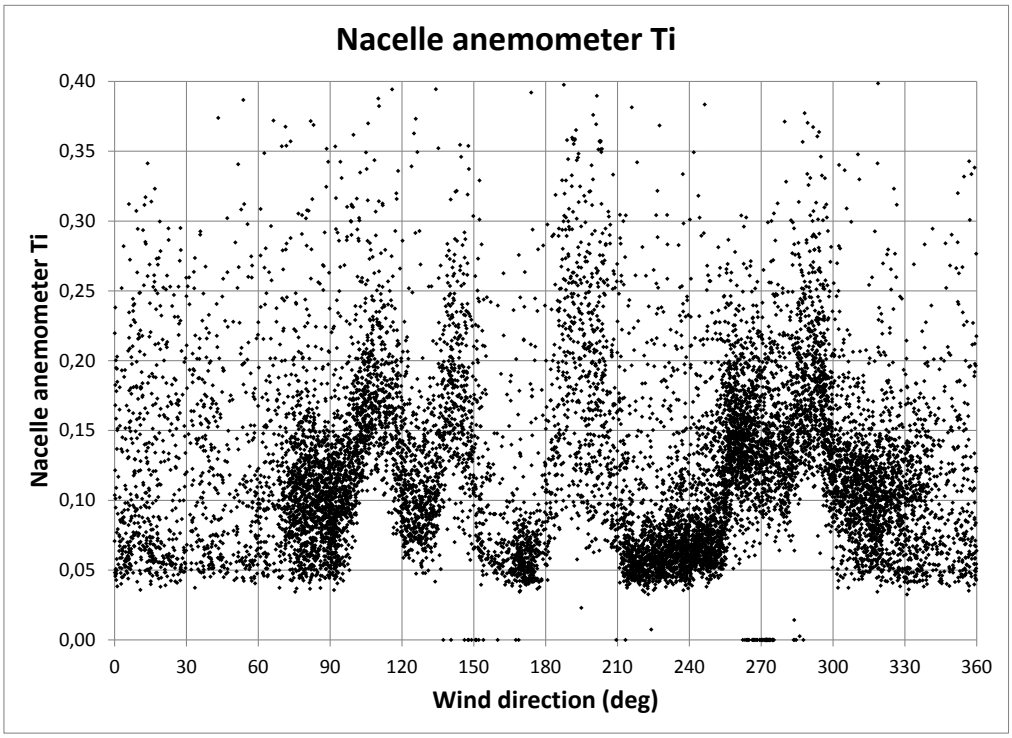

Figure 40 Turbulence intensity measured by nacelle anemometer in all directions

3.9 V80 power curve measurements

The power curve of the V80 wind turbine was analysed for the three different wind speed methods, spinner anemometer, mast cup anemometer and nacelle anemometer. No correction for air density was made on the power. The power curve measured with the spinner anemometer, mast cup anemometer and the nacelle anemometer are shown with 10min and 30sec data in Figure 41 and Figure 42, Figure 43 and Figure 44, and in Figure 45 and Figure 46, respectively.

The spinner anemometer and the nacelle anemometer are both able to measure the wind from all directions without being disturbed by wind turbine wakes like the mast wind measurements. Power curve measurements from all wind directions for the spinner anemometer and the nacelle anemometer are shown in Figure 47 and Figure 48.

The power curve measured with the spinner anemometer and the mast cup anemometer without induction correction is shown in Figure 49, and the corresponding plot, where induction is corrected for with the induction function, is shown in Figure 50.

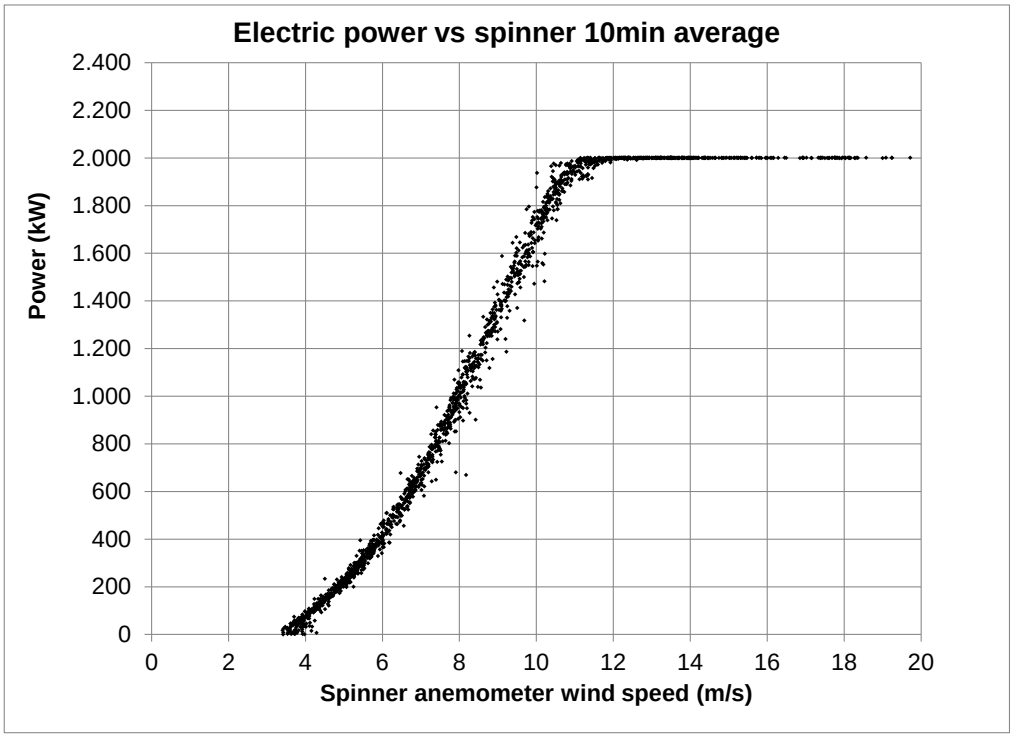

Figure 41 Power versus spinner wind speed with 10min averages for free wind sector 212°-252°

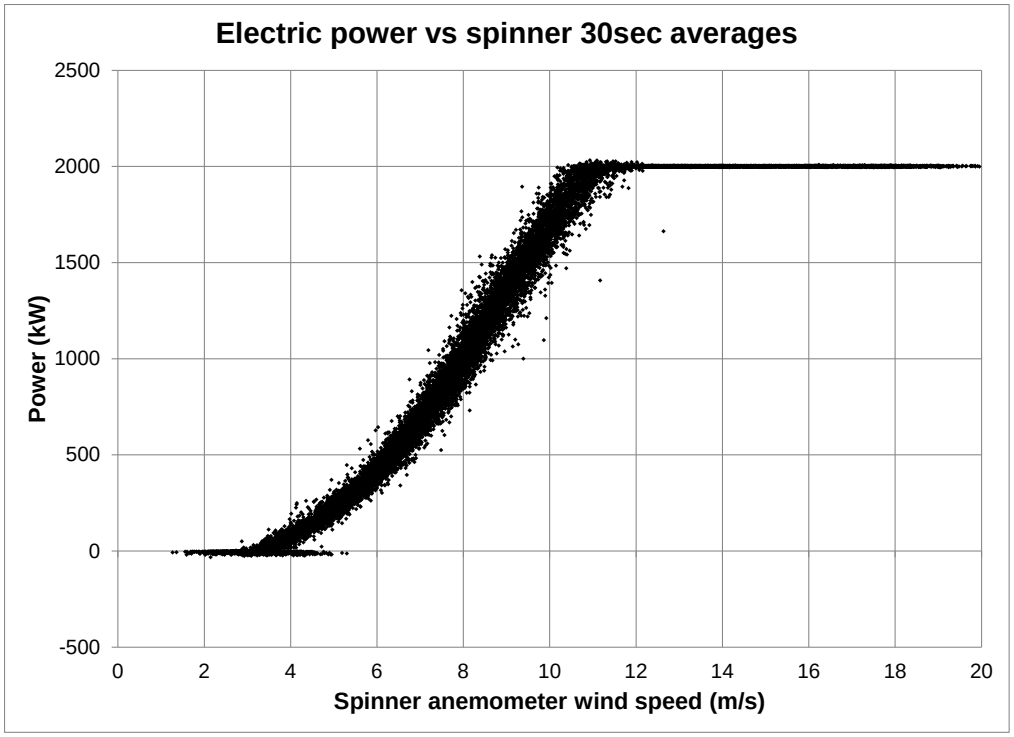

Figure 42 Power versus spinner wind speed with 30s averages for free wind sector 212°-252°

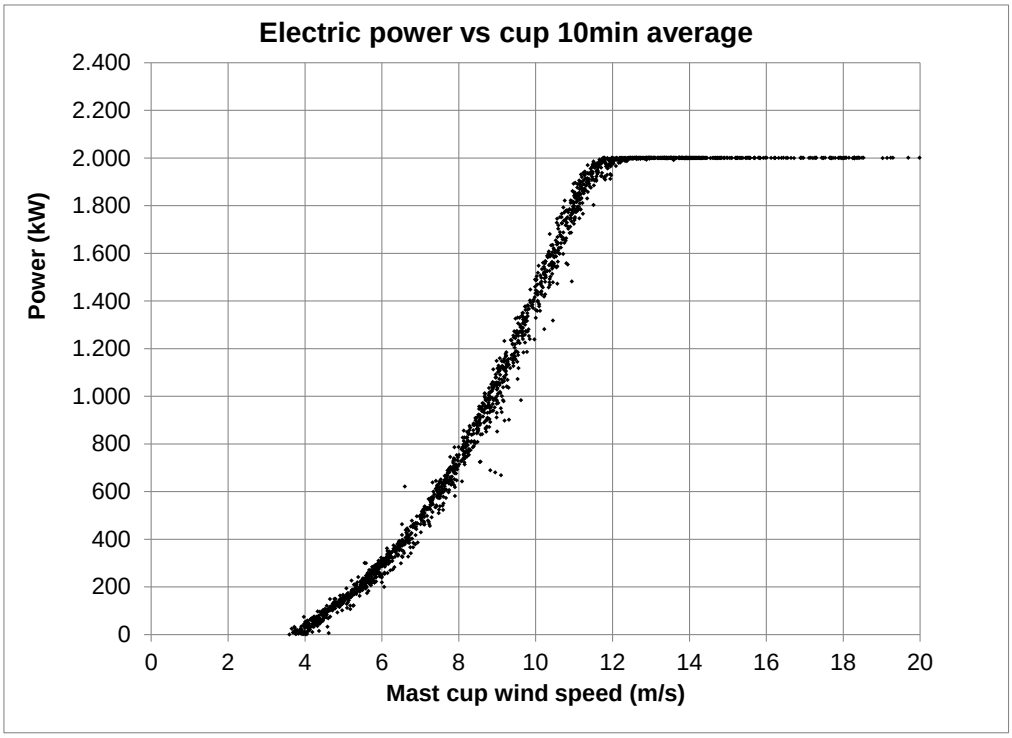

Figure 43 Power versus mast cup wind speed with 10min averages for free wind sector 212°-252°

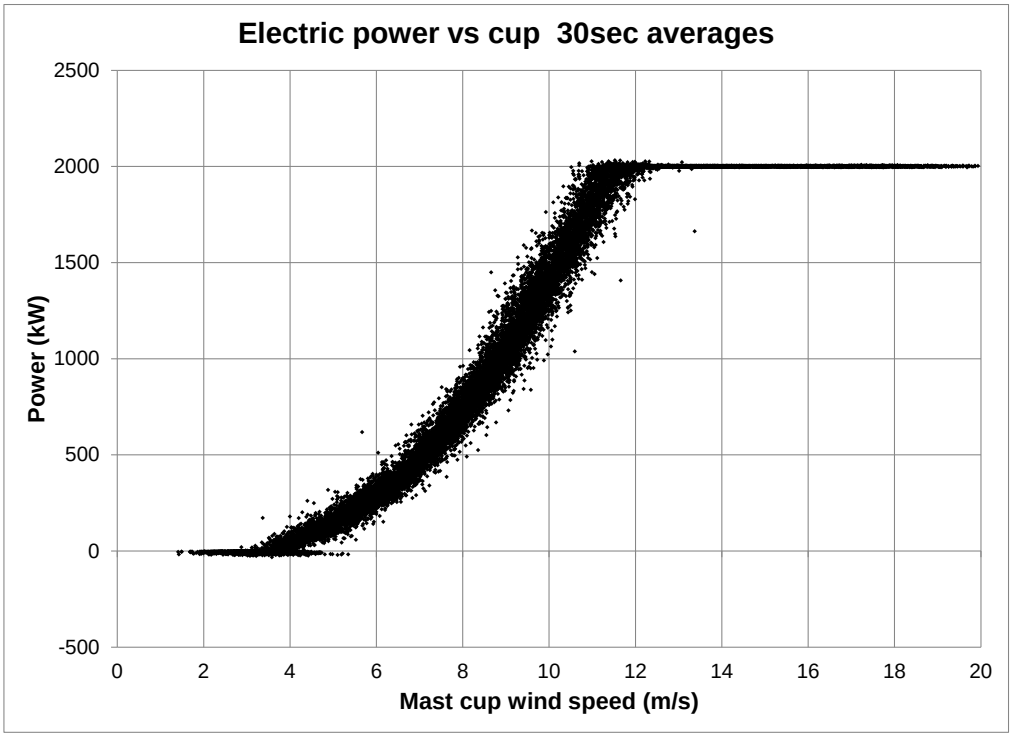

Figure 44 Power versus mast cup wind speed with 30s averages for free wind sector 212°-252°

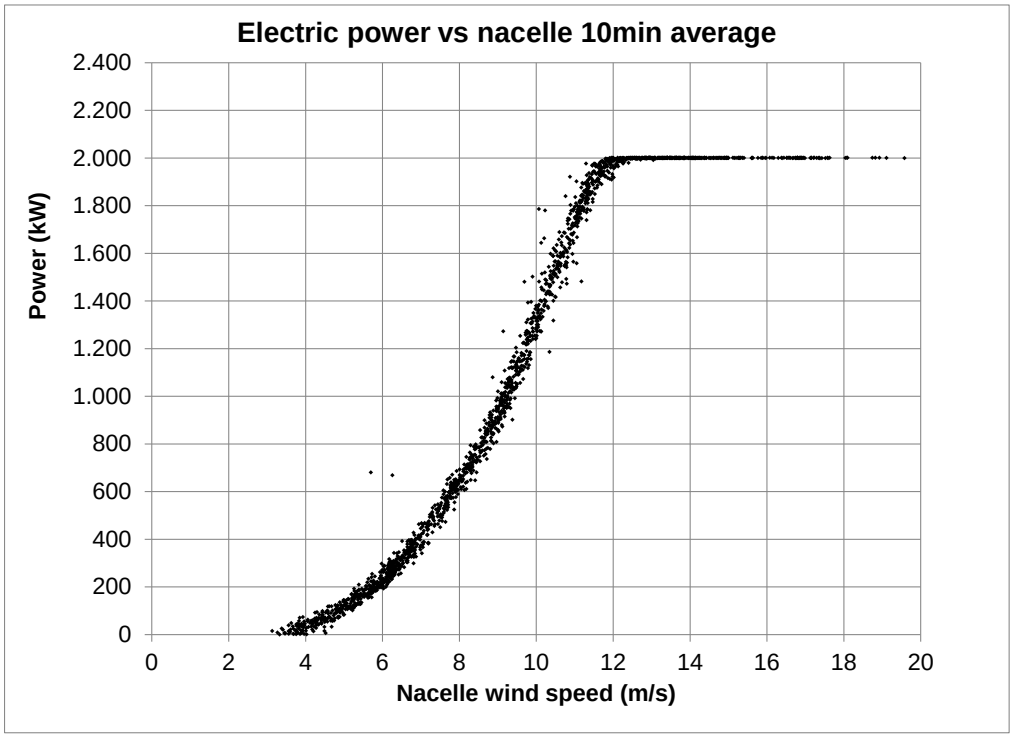

Figure 45 Power versus nacelle wind speed with 10min averages for free wind sector 212°-252°

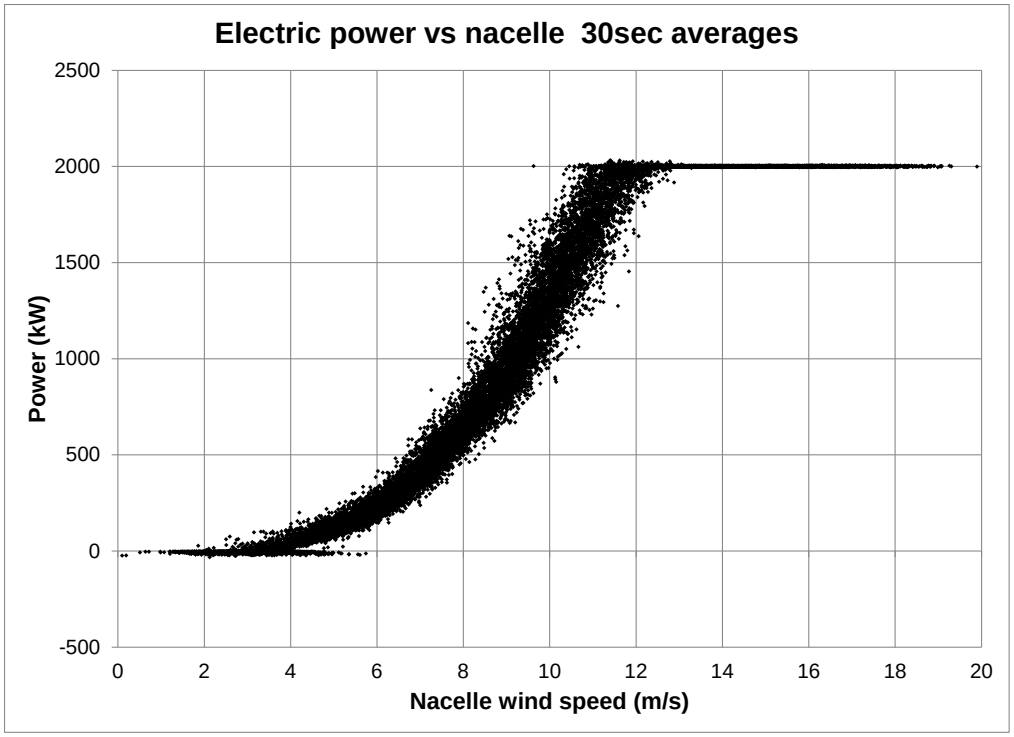

Figure 46 Power versus nacelle wind speed with 30s averages for free wind sector 212°-252°

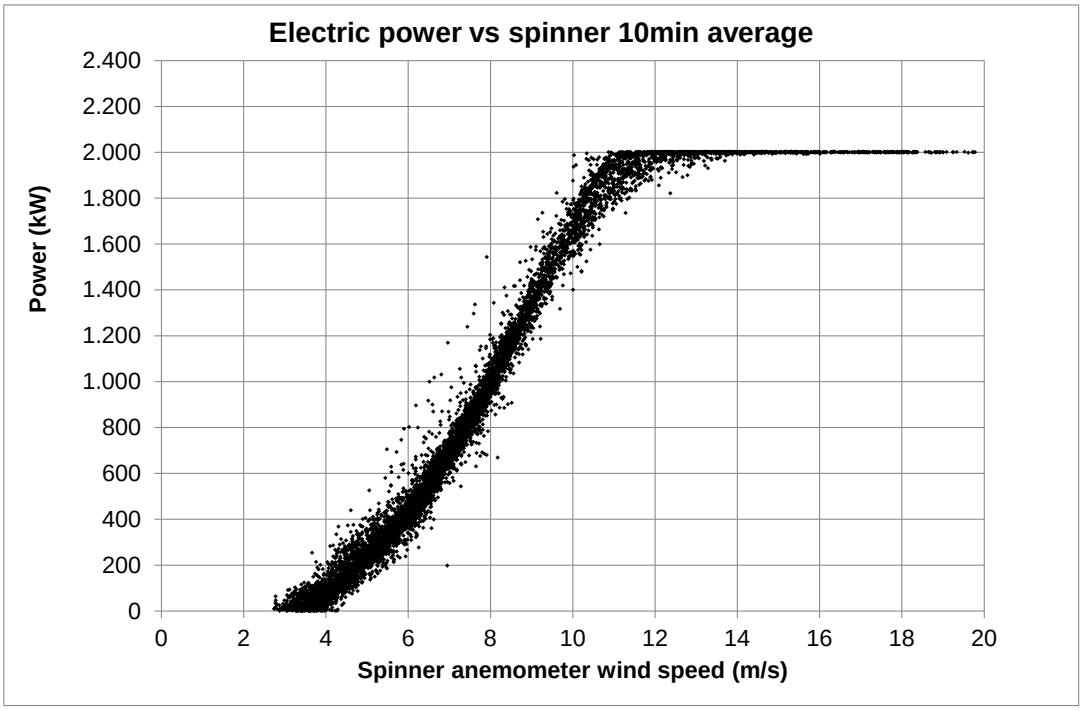

Figure 47 Power versus spinner wind speed with 10min averages for all wind directions

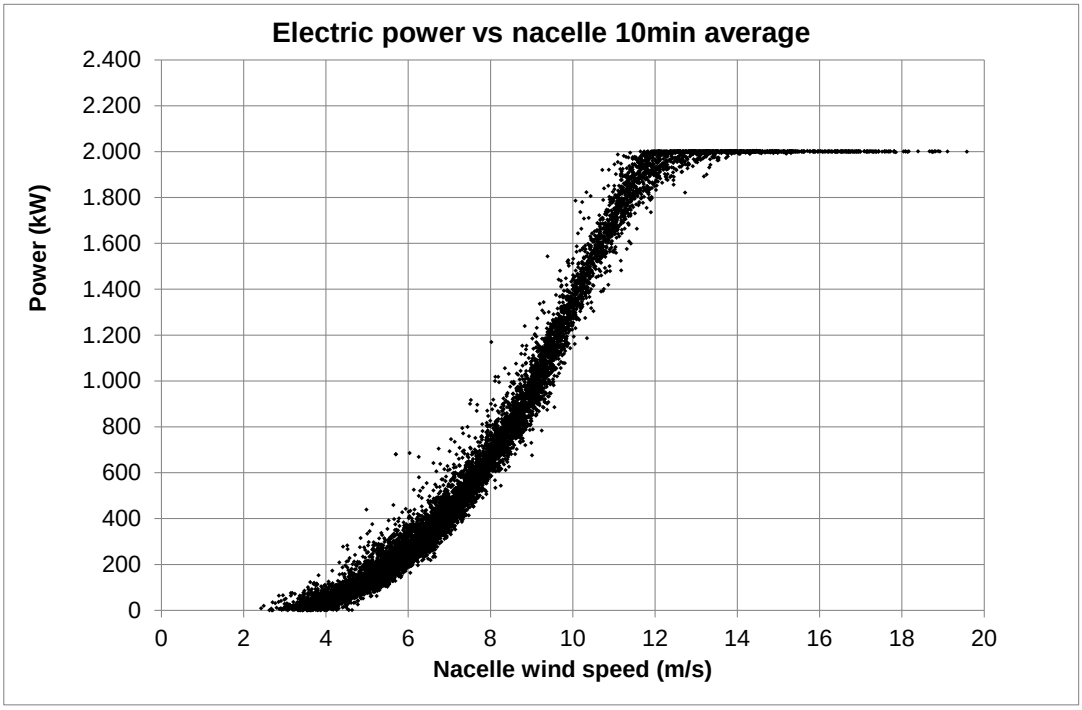

Figure 48 Power versus nacelle wind speed with 10min averages for all wind directions

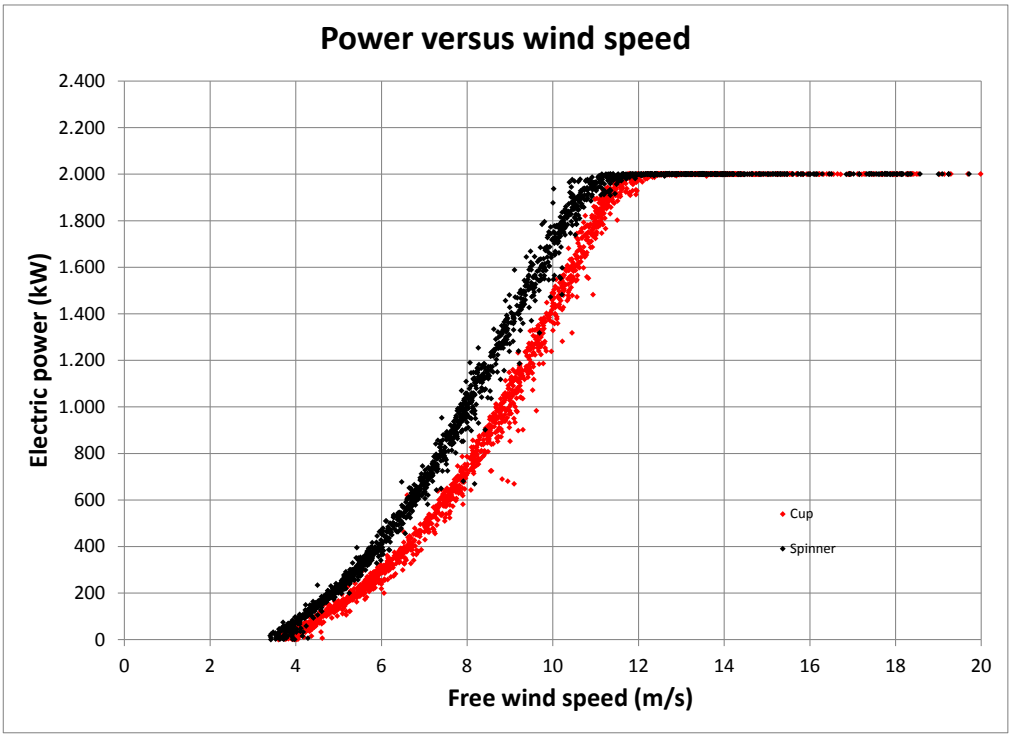

Figure 49 Power curves measured with the spinner anemometer and the mast cup anemometer without induction correction

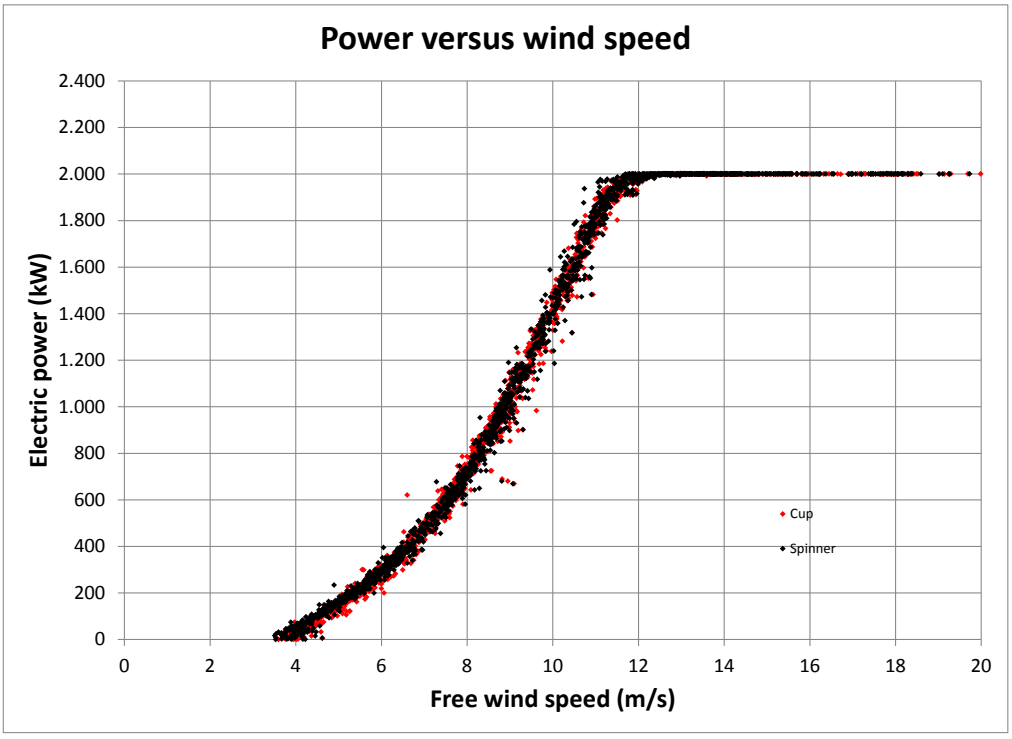

Figure 50 Power curves measured with the spinner anemometer and the mast cup anemometer where induction is corrected for with the induction function

3.10 Power gain of Horns Reef 1 wind farm with optimized yawing

The Horns Reef 1 wind farm has 80 V80 wind turbines, similar to the wind turbine in Tjæreborg wind farm, see Figure 51. It has been operated for several years and a database of SCADA data has been gathered. These data consists of power data, nacelle wind speed and wind direction data, and yawing direction data. A parametric analysis was made based on yawing directions, and position of the turbines in the wind farm. The yawing directions showed quite large variations, indicating that yaw errors could be significant. However, the large variations in yaw direction are not due to yaw errors. It is assumed that they are due to the yaw direction sensors not being calibrated relative to each other and also being unstable. This is confirmed when looking at longer term statistics. Thus it was concluded that it was not possible to estimate yaw errors from SCADA data.

Figure 51 The Horns Reef 1 wind farm layout of 80 Vestas V80 wind turbines

An estimate of the power losses of the Horns Reef 1 wind farm, due to yaw error was made with the use of the V80 onshore measurements, see Figure 29. It was assumed that all wind turbines in the wind farm had the same yaw error as the one measured on the V80 onshore turbine, being 11° in average, see Figure 29. The energy loss due to yaw error was calculated according to the model developed by Højstrup [14]. The Højstrup model assumes the power of a wind turbine with yaw error reduced with the power corresponding to the reduced wind speed perpendicular to the wind turbine. This will cause the power curve to shift to the right, and to reduce the power with varying $\cos^n$ relationship as function of wind speed. As a result the annual energy production reduction for annual wind speeds of 6-7m/s is $\cos^2$ shaped, see Figure 52. For higher annual average wind speeds the power loss is less. Assuming an average wind speed of 9.7m/s of the Horns Rev wind farm the energy loss is estimated by extrapolation to 2.04%.

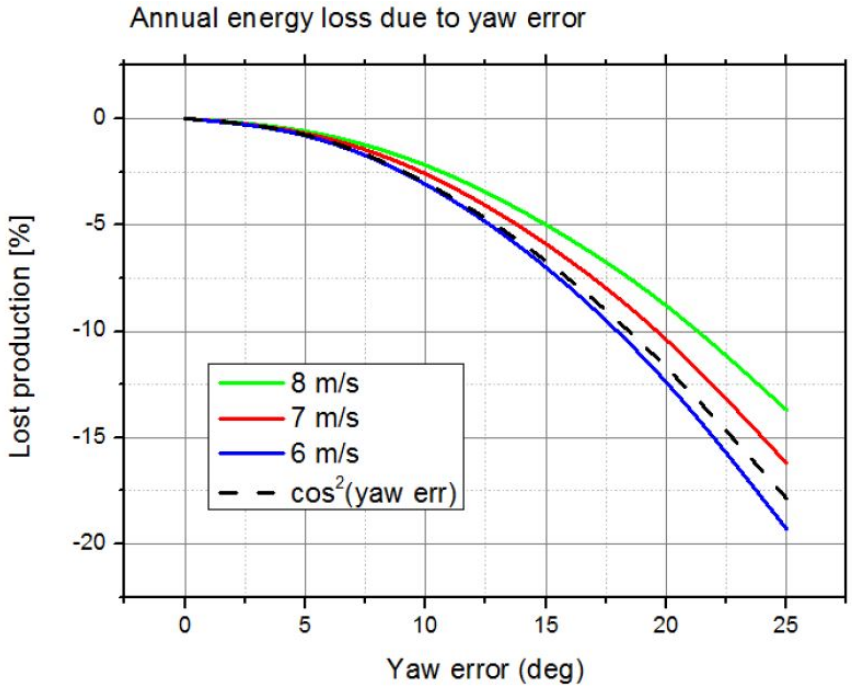

Figure 52 Annual energy loss model of Højstrup, see ref 14

4. Yaw error measurements in Vedersø Kær wind farm

4.1 Vedersø Kær wind farm site

In order to investigate the improvement of power performance of a wind farm by means of spinner anemometry nine spinner anemometers were mounted on wind turbines in the Vedersø Kær wind farm, see Figure 53. The wind farm consists of 10 wind turbines in two rows of five, directed from southwest to northeast. The wind turbines are all NEG Micon 1,5MW wind turbines with hub height 68m and rotor diameter 64m.

Figure 53 Location of Vedersø Kær wind farm with 10 NEG Micon 1,5MW wind turbines with hub height 68m and rotor diameter 64m. The wind turbines are located on two rows directed from southwest to northeast

Yaw errors were measured with spinner anemometers in the period from end of June to medio November 2012. The shortest measurement period on a wind turbine was 24 days and the longest was 4 month 9 days. The measurements were performed with the default spinner anemometer constants $K_1 = K_2 = 1$. Calibrations made by ROMO Wind of the correction factors resulted in the calibrated constants $K_1 = 0.558$ and $K_2 = 0.68$. Wind speed measurements were calibrated linearly, see chapter 5, during normal operation. This means that the K_1 constant is determined while induction in average is reducing the wind speed at the spinner location. Yaw measurements were calibrated linearly, see chapter 5.

4.2 Yaw error measurements in Vedersø Kær wind farm

The results of the yaw measurements in Vedersø Kær wind farm are shown in Figure 54 to Figure 62. The average yaw errors are summarized in Table 2.

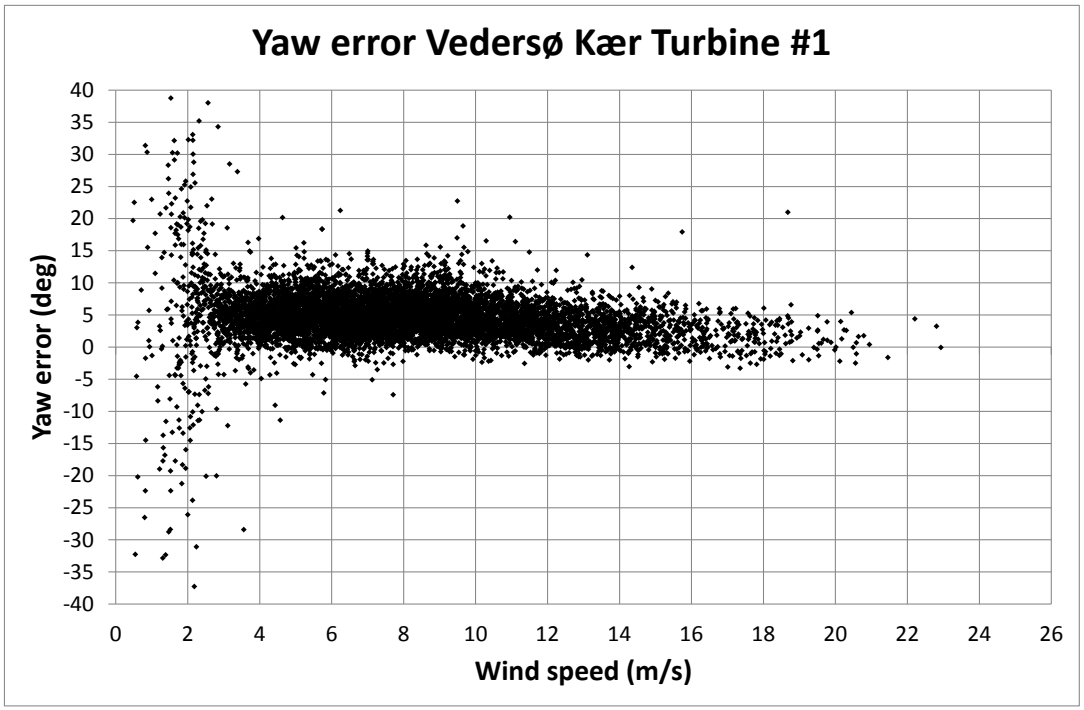

Figure 54 Yaw error measurements on wind turbin #1 in Vedersø Kær wind farm

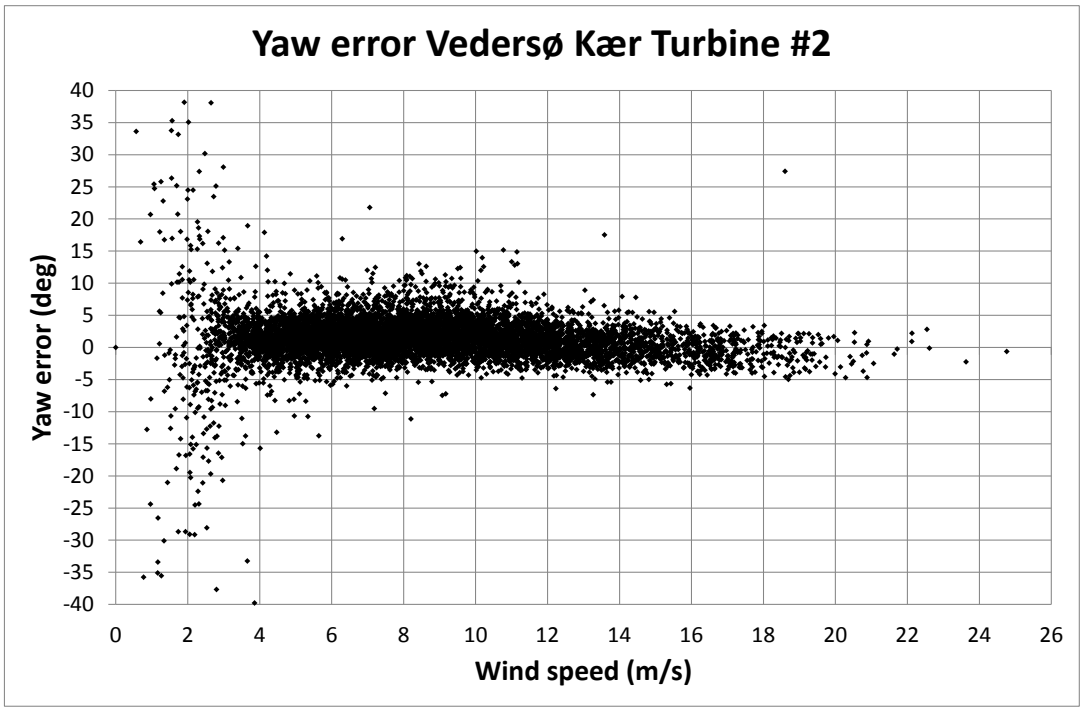

Figure 55 Yaw error measurements on wind turbin #2 in Vedersø Kær wind farm

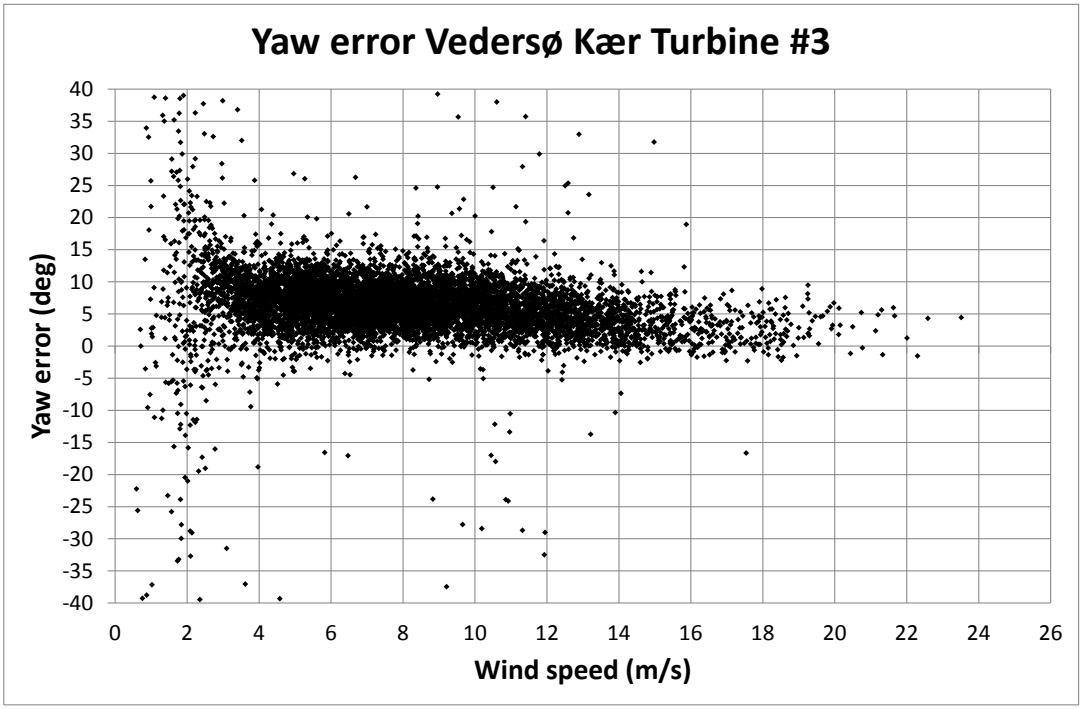

Figure 56 Yaw error measurements on wind turbin #3 in Vedersø Kær wind farm

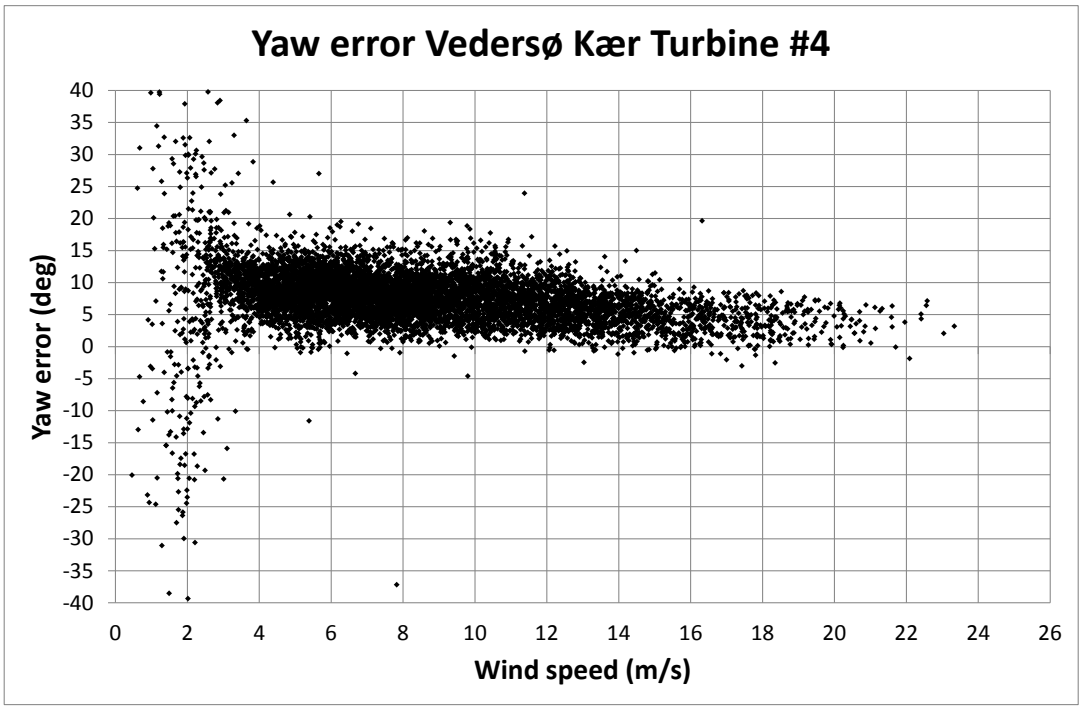

Figure 57 Yaw error measurements on wind turbin #4 in Vedersø Kær wind farm

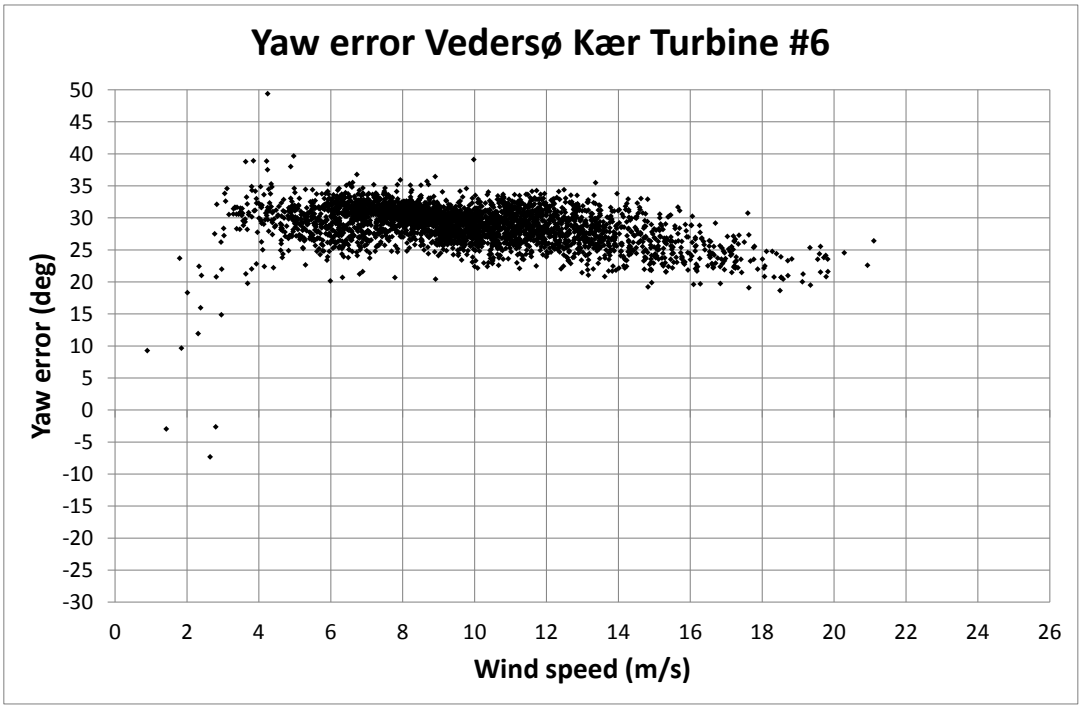

Figure 58 Yaw error measurements on wind turbin #6 in Vedersø Kær wind farm

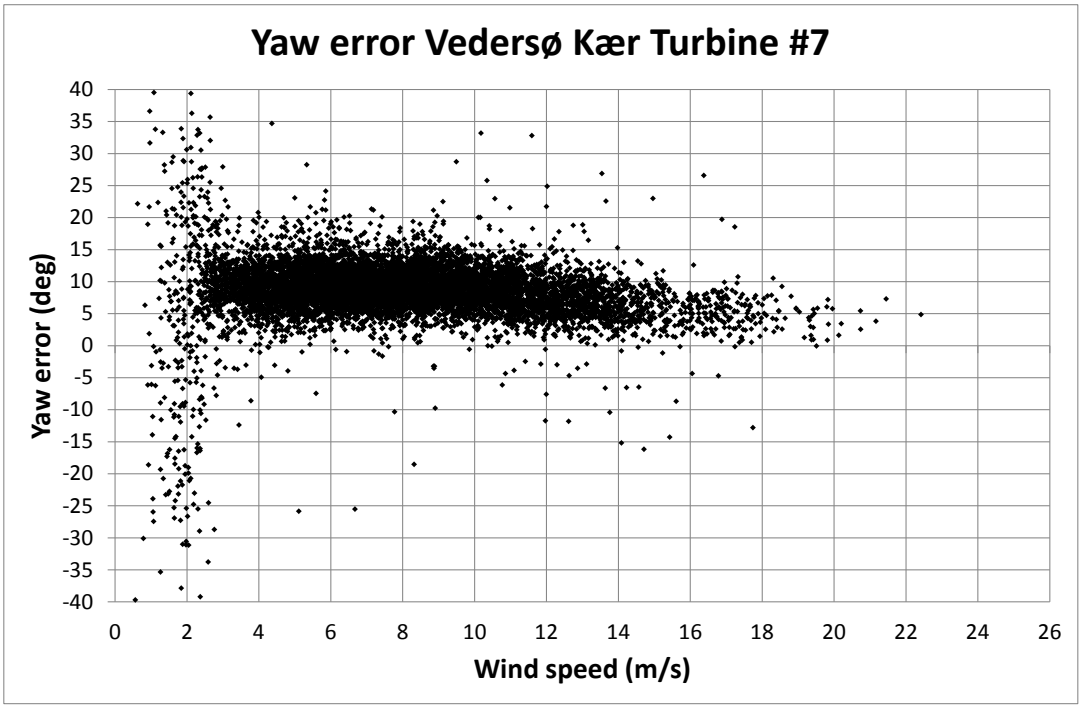

Figure 59 Yaw error measurements on wind turbin #7 in Vedersø Kær wind farm

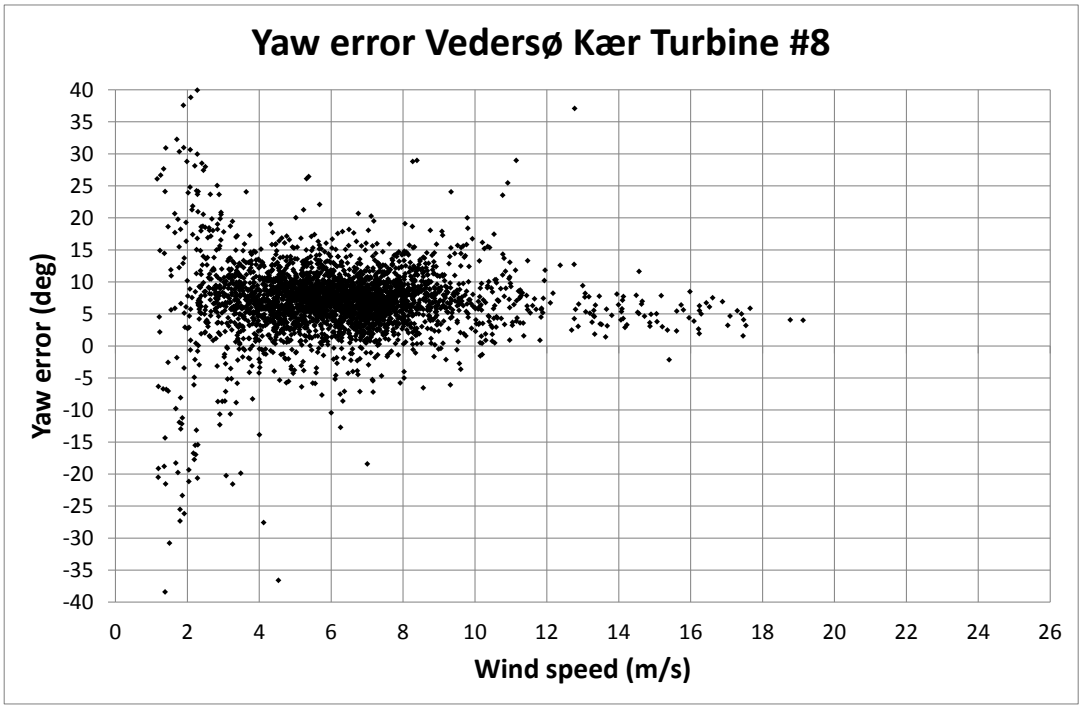

Figure 60 Yaw error measurements on wind turbin #8 in Vedersø Kær wind farm

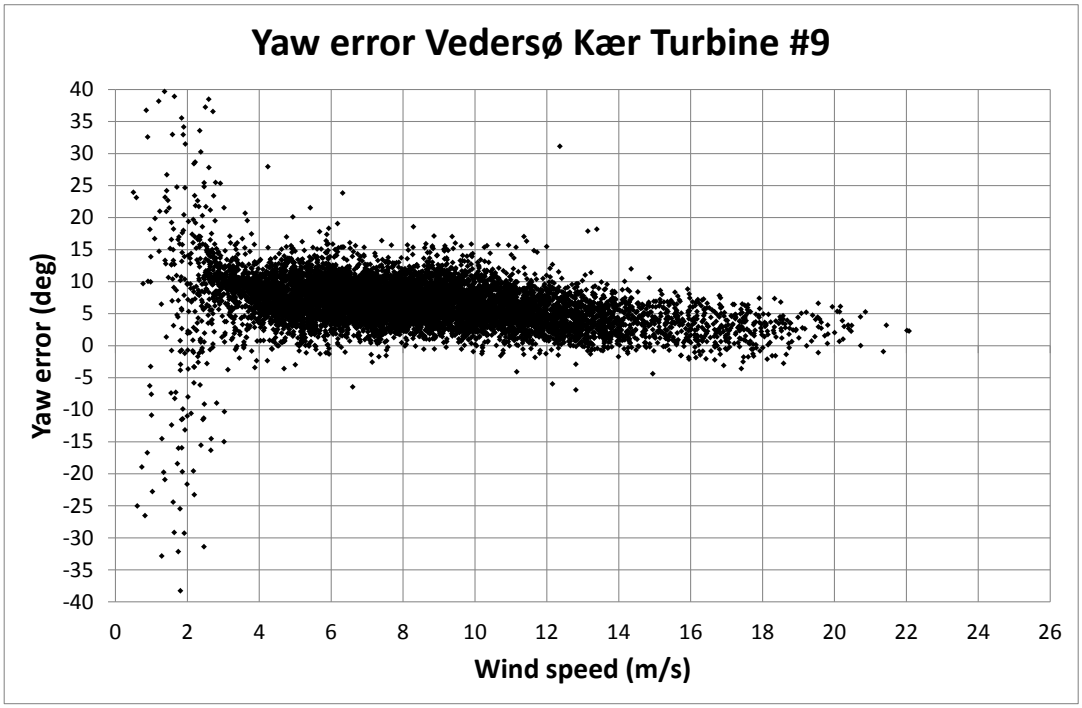

Figure 61 Yaw error measurements on wind turbin #9 in Vedersø Kær wind farm

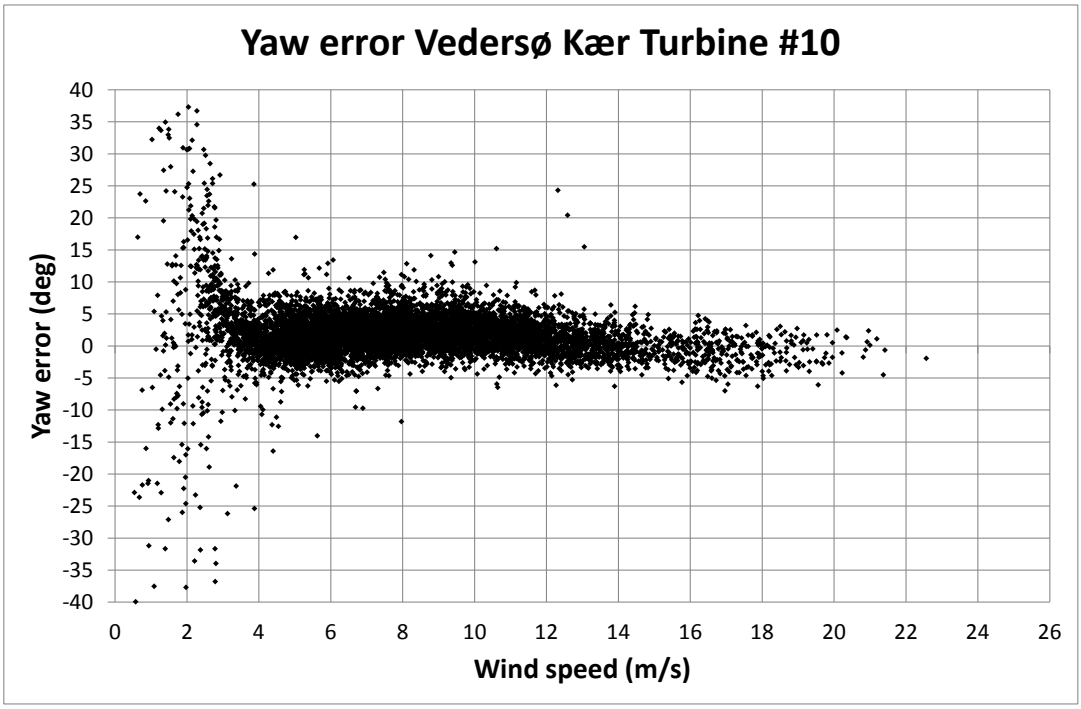

Figure 62 Yaw error measurements on wind turbin #10 in Vedersø Kær wind farm

4.3 Power loss of Vedersø Kær wind farm with yaw errors

The yaw errors measured on the nine wind turbines in Vedersø Kær wind farm indicate that there is a potential power gain possible with optimized yawing. The average yaw errors for each of the nine wind turbines in the wind speed range 4-12m/s are listed in Table 2. Assuming the same Højstrup power loss model [14] as for the Horns Rev wind farm, and an annual average wind speed of 7.2m/s the estimated losses are as shown in Table 2.

The summarized energy loss is calculated as 3.15% which corresponds to 1039MWh in annual energy production. The power loss, though, is very much concentrated on wind turbine no. 6 with 28.9° yaw error. If we omitted this wind turbine as well as no. 5 and only consider the eight wind turbines the energy loss (and potential energy gain) is 0.98%.

ROMO Wind made another analysis. They measured the power curve with the nacelle anemometer before and after adjustments of the yaw errors. They found in average a gain in AEP of 2.5% after wind vane adjustments (with wind turbine no. 6 initially adjusted to 9.7°). Vattenfall made a separate measurement with their SCADA system. They measured the energy of each turbine of the wind farm in a period before wind vane adjustment and in another period after wind vane adjustment. They normalized the energy production with turbine number 2, which had a yaw error of only 1.4°, and where almost no adjustment of the wind vane was made. They found an increase of AEP of 2.6% after wind vane adjustments.

These three ways of assessment of annual energy loss due to yaw error deviate significantly. The assessment of ROMO and Vattenfall seems to agree quite well while the Højstrup method gives lower results. The way that the Højstrup method was implemented, though, was with average yaw error. The result would be somewhat higher if the power loss for each 10min wind

speed data set was calculated. A more detailed assessment is required in order to investigate the specific cause of the differences.
°°

Table 2 Average yaw errors of wind turbines in Vedersø Kær wind farm and annual energy losses

Wind turbine	Average yaw error	Annual energy loss	Average yaw error ROMO	Annual energy loss ROMO (nacelle anem)
No.	(°)	(%)	(°)	(%)
1	4.6	0.56	4.8	2.6
2	1.4	0.05	1.6	0.5
3	6.4	1.08	6.6	2.2
4	7.7	1.55	7.9	3.7
5*	0	0	0	0
6	28.9	20.55	9.7	3.9
7	8.7	1.98	9.2	3.0
8	7.2	1.36	7.5	3.7
9	6.7	1.18	6.8	3.8
10	1.8	0.09	1.8	-0.8
* not measured		Ave 3.15		Ave 2.51

5. Errors in linearizing calibration corrections

The spinner anemometer algorithm is not linear. The larger the angle of attack to the shaft axis the higher the error in using a linear correction of data measured with default $K_1 = K_2 = 1$ values. In the analysis of both the Tjæreborg and Vedersø Kær data these default K values were used and a linearized calibration of the data was made. Yaw errors were corrected with the formula:

$$\gamma = \gamma_d / F_\alpha$$

Here γ is the yaw error, the subscript d stand for default, and the F_α conversion factor is the slope of the regression curve of the γ values to the γ_d values for the yaw calibration data where the wind turbine was yawed in and out of the wind. However, according to the exact spinner algorithm the accurate correction should be:

$$\alpha = A\tan(\tan\alpha_d / F_\alpha)$$

Here α denotes the inflow angle to the shaft axis and is a combination of the yaw error γ and the flow inclination angle β (added the tilt angle δ) and the F_α conversion factor is related to the K constant values, the F conversion factors and the α inflow angles as:

$$F_\alpha = \frac{K_\alpha}{K_{\alpha,d}} = \frac{F_2}{F_1} = \frac{K_2 K_{1,d}}{K_1 K_{2,d}} = \frac{\tan\alpha_d}{\tan\alpha}$$

This is based on the relations:

$$K_\alpha = \frac{K_2}{K_1} \qquad F_1 = \frac{K_1}{K_{1,d}} \qquad F_2 = \frac{K_2}{K_{2,d}}$$

The error in using the linearized conversion rather than using the spinner anemometer algorithm is shown in Figure 63. The angle error is shown in percent for different F_α values and actual inflow angles α. $F_\alpha = 1.22$ corresponds to the Vedersø Kær measurements while $F_\alpha = 1.0$ corresponds to the Tjæreborg measurements. The overestimation error for $\alpha = 10°$ is 0.06° while the error for $\alpha = 30°$ is 1.4°. The use of the accurate conversion formula makes the conversion significantly more complex. For simplicity, and because the error is rather small for small inflow angles, the linearized conversion was used for all calculations in this report.

Wind speeds were corrected with the formula:

$$U = U_d / F_1$$

Here the F_1 conversion factor is the slope of the regression curve of the mast cup wind speed U values to the spinner wind speed U_d values for the wind speed calibration data. However, according to the exact spinner algorithm the accurate wind speed correction should be:

$$U = U_d \frac{1}{F_1} \frac{\cos\alpha_d}{\cos\alpha}$$

The linearization error on the wind speed is seen to be independent of the F_1 value and it is only dependent on the un-linearity of the flow angles, and thus the F_α value. The error in using the linearized conversion for the wind speeds is shown in Figure 64.

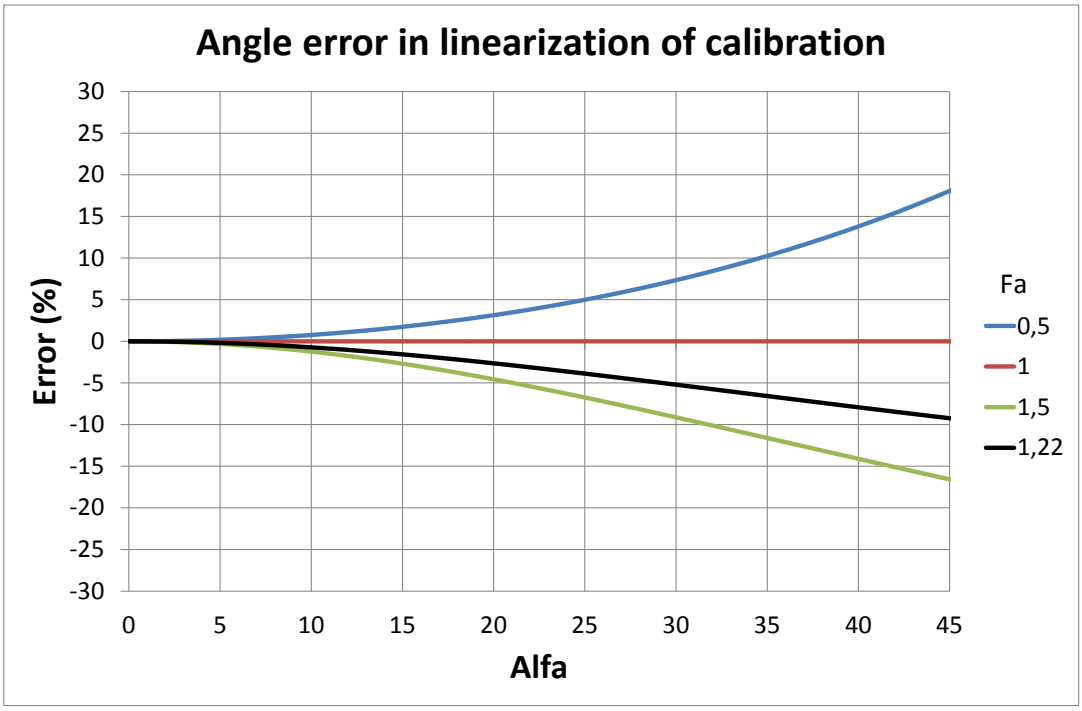

Figure 63 Angle error in conversion from default inflow angles α_d to calibrated inflow angles α with conversion factor F_α. $F_\alpha = 1.22$ corresponds to Vedersø Kær data and $F_\alpha = 1$ to Tjæreborg data

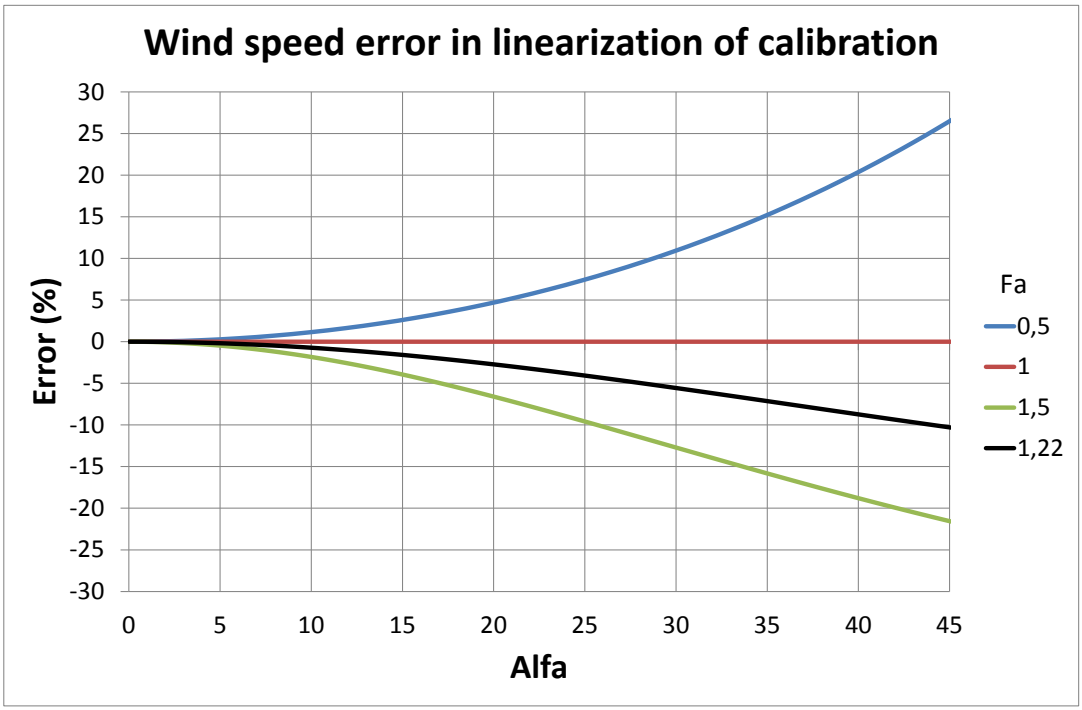

Figure 64 Wind speed error in conversion from default wind speed U_d to calibrated wind speed U with conversion factor F_α. $F_\alpha = 1.22$ corresponds to Vedersø Kær data and $F_\alpha = 1$ to Tjæreborg data

6. Commercialization of the spinner anemometer

An objective of the project was to commercialize the spinner anemometer. The focus on this was in the beginning to make licence agreements with sonic sensor manufacturers. One sonic sensor manufacturer was from the beginning interested in the concept and saw a large market potential.

6.1 Metek licence

Metek produced the prototype spinner anemometers for Risø/DTU. After some research projects where the concept was tested and proved to work well a licence agreement was made with Metek. The licence agreement was for a limited number of spinner anemometers produced and installed. Metek, however, had not a substantial market share on nacelle sensors on beforehand. The focus of Metek products is in meteorology. Penetration for a newcomer on the nacelle sensor market is very difficult. This is due to conservatism regarding sensor robustness, and lifetime considerations.

6.2 ROMO Wind acquisition of the spinner anemometer patent

A new player in the field, ROMO Wind, with senior experts in wind energy, was introduced to the spinner anemometer, and they found the technology attractive for their business plans. After negotiations ROMO Wind acquired the patent of the spinner anemometer at the end of 2011. They continued to use Metek as prime supplier of spinner anemometers. Together they implemented improvements of the spinner anemometer to make it ready for the commercial market. DTU supported ROMO Wind with technical diligence to transfer the technology to the commercial company. They entered the SpinnerFarm project to take over some of the responsibilities for wind farm measurements and they supported the measurements in the Vedersø Kær wind farm as a substitute for the Horns Rev 1 Wind farm measurements.

6.3 ROMO Wind marketing

ROMO Wind established their company in Aarhus and hired 15 people, many of these experienced senior experts in wind energy. The ROMO Wind web site, www.romowind.com, shows spinner anemometry being their primary product for their business concept on energy efficiency improvements. ROMO Wind has in their marketing made contact with large parts of the wind energy community, and they have acquired a good understanding of their market position. They are developing new products in order to connect spinner anemometry technology to control of wind turbines, and are continuing their development in a cooperation with DTU in a new EUDP project called “iSpin”.

7. Dissemination

The results of the project have been disseminated in reports, papers, article and conferences. Contributions were made to the EWEA conferences 2010, 2011 and 2013 [10,12, 14]. An article was made to WindTECH International [13], and an article was submitted to Wind Energy journal 2013 [15].

8. Conclusions

The project resulted in an improvement of the spinner anemometer technology and in verifying new measurement features of the instrument. Yaw errors on a test wind turbine and on nine wind turbines in an onshore wind farm was determined and potential annual energy gains were estimated.

The hardware was improved by a more powerful microprocessor and heating was added to the sonic sensor arms plus a range of smaller redesigns which resulted in a more robust instrument. The software was revised with an improved internal calibration procedure. The improved system was tested on a 2MW test wind turbine at Tjæreborg wind farm. Measurements on the test turbine included calibration of K factors, for inflow angle measurements and for wind speed measurements. The nacelle transfer function was determined with an external mast, and the nacelle transfer function was identified as a wind speed induction function for the induction in the center of the rotor. Measurements of yaw error, inflow angle and turbulence intensity, and measurements of power performance were made, and the measurements were compared with the mast cup anemometer and wind vane and the nacelle anemometer. The measurements of turbulence intensity showed that the standard deviations measured by the spinner anemometer and the mast cup anemometer match very well. However, the wind speed measured by the spinner anemometer is reduced about 11% as maximum by the induction in the center of the rotor. This results in turbulence intensity measurements by the spinner anemometer that is overestimated by about 11% compared to the mast cup anemometer. When applying the induction function to the spinner anemometer wind speed, the turbulence intensity compares quite well with the mast cup turbulence.

The average yaw error measurement of the V80 turbine at Tjæreborg was 11°. With an estimated average wind speed of the Horns Rev wind farm of 9.7m/s and the average yaw error measured on the onshore wind turbine the estimated potential energy gain using the Højstrup model was found to 2.04%.

Nine spinner anemometers were mounted on nine out of ten wind turbines in the Vedersø Kær wind farm and statistics of yaw error measurements were determined. The yaw error averages in the wind speed range 2-13m/s of each wind turbine were measured to be: 4.6°, 1.4°, 6.4°, 7.7°, 28.9°, 8.7°, 7.2°, 6.7° and 1.8°. The highest yaw error of 28.9°was quite substantial. With an estimated average wind speed of the wind farm of 7.2m/s and using the average yaw error of each wind turbine and the Højstrup energy loss model, the energy losses were estimated at: 0.56%, 0.05%, 1.08%, 1.55%, 20.55%, 1.98%, 1.36%, 1.18% and 0.09%. The average energy loss is 3.15%, but if omitting the largest average yaw error of 28.9° the energy loss is estimated at 0.98%. ROMO measured the power curves before and after adjustments with use of the nacelle anemometer (the yaw error of 28.9° was first adjusted down to 9.7°) and found an energy gain of 2.5% after adjustments of wind vanes. Vattenfall made a separate measurement with their SCADA system and found an energy increase of 2.6%. The measurements made by ROMO and Vattenfall on the Vedersø Kær wind farm agreed with each other, while the estimates made with the Højstrup model were significantly lower using the average yaw error value. The reason for the low values found with use of the Højstrup model should be found in the unlinearity of the $\cos^n$ function. One has to consider the variations of the 10min averaged yaw errors. The value of the results presented here with average yaw errors has thus a limited value. For a proper comparison the variation of yaw errors must be taken into account.

References

1. Pedersen TF, Madsen HA, Møller R, Courtney, M, Sørensen NN, Enevoldsen P, Egedal P, “Spinner Anemometry – An Innovative Wind Measurement Concept”, EWEC2007 Milan, paper and poster (poster award)

2. Sørensen NN, Pedersen TF, CFD computation around wind turbine spinner and nacelle, Risø-I-2579(EN), June 2007

3. Pedersen TF, Sørensen N, Enevoldsen P, "Aerodynamics and Characteristics of a Spinner Anemometer", International conference: The science of making torque from wind, Lyngby (DK), 28-31 Aug 2007 J. Phys.: Conf. Ser. 75 012018 (9pp)

4. Spinder Anemometri, presentation Vinddag 2007, Risø DTU

5. Pedersen TF, Vita L, Sørensen NN, Enevoldsen P, “Operational Experiences with a Spinner Anemometer on a MW Size Wind Turbine”, EWEC2008, Bruxelles

6. Pedersen TF, Vita L, Sørensen NN, Enevoldsen P, “Optimization of Wind Turbine Operation by Use of Spinner Anemometer”, Risø-R-1654(EN), 2008

7. Pedersen TF, Den Intelligente Spinder, presentation , Risø Vinddag 2008

8. Pedersen TF, Risø Spinner Anemometer, Prototype 2, Installation and Calibration and Quality of Signal Output, Risø-I-2779, October 2008 (Not published)

9. Weich G, Spinner Anemometer User Manual 05-01-2009, Metek

10. Pedersen TF, Gottschall J, Kristoffersen JR, Dahlberg J-Å, Christiansen W, Weich G, Wedell-Hansen J, Application of Spinner Anemometry in Yaw Aligment Control, poster 251, EWEA2010 conference, Warzaw 2010

11. Pedersen TF, Spinner anemometry – basic principles for application of the technology, Risø-I-2968(EN)(rev.1), September 2010 (Not published)

12. Pedersen TF, Gottschall J, Kristoffersen JR, Dahlberg J-Å, Yawing and performance of an offshore wind farm, EWEA2011 Brussels, 2011, paper and poster 094

13. Højstrup J, ROMO Wind Spinner Anemometer, WindTECH International, November/December 2012, Volume 8 No. 8

14. Højstrup J, Nielsen SD, Hansen JK, Lauritsen JL, Maximize Energy Production by minimizing Yaw Misalignment. Large Scale Field Deployment of Spinner Anemometer, EWEA2013 Vienna, Poster 0162 (poster award)

15. Pedersen TF, Demurtas G, Calibration of a spinner anemometer for yaw error measurements, article submitted to Wind Energy journal 2013

Acknowledgements

A great acknowledgement to Vattenfall A/S is given for the financial support to this project, and for the permission to make the tests on the Tjæreborg wind turbine and the Vedersø Kær wind farm. Also acknowledgement for great partnership and flexibility in selection of wind farm site for the project and in accepting ROMO Wind A/S as new partner in the project.

A great acknowledgement to ROMO Wind A/S first of all for achieving the spinner anemometer technology form DTU and for their flexible integration into this project. ROMO Wind has over the last part of the project made a tremendous effort on marketing of the spinner anemometer technology on the wind energy market. The cooperation with ROMO Wind has been a real pleasure.

A great acknowledgements also to Metek GmbH who originally made the prototype spinner anemometers and also supplied this project with spinner anemometers, and who continues to be supplier of spinner anemometers to ROMO Wind with their sonic anemometer technology. Cooperation with Metek on development of the spinner anemometer concept has really been a pleasure.

DTU Vindenergi er et institut under Danmarks Tekniske Universitet med en unik integration af forskning, uddannelse, innovation og offentlige/private konsulentopgaver inden for vindenergi. Vores aktiviteter bidrager til nye muligheder og teknologier inden for udnyttelse af vindenergi, både globalt og nationalt. Forskningen har fokus på specifikke tekniske og videnskabelige områder, der er centrale for udvikling, innovation og brug af vindenergi, og som danner grundlaget for højt kvalificerede uddannelser på universitetet.

Vi har mere end 230 ansatte og heraf er ca. 60 ph.d. studerende. Forskningen tager udgangspunkt i 9 forskningsprogrammer, der er organiseret i tre hovedgrupper: vindenergisystemer, vindmølleteknologi og grundlag for vindenergi.

Technical University of Denmark
DTU Vindenergi
Frederiksborgvej 399
Bygning 125
4000 Roskilde
Telefon 45 25 25 25
info@vindenergi.dtu.dk
www.vindenergi.dtu.dk